Review of designs and flight control techniques of hybrid and convertible VTOL UAVs

Guillaume Ducard, Mike Allenspach

Version of Record: https://www.sciencedirect.com/science/article/pii/S1270963821005459
Manuscript_6110fdc4f137898975bd5e96b3b8d7ff

Review of Designs and Flight Control Techniques of Hybrid and Convertible VTOL UAVs

Guillaume J.J. Ducard[a,c], Mike Allenspach[b,c]

[a]*I3S, University Côte d'Azur, CNRS, 06903 Sophia Antipolis, France*
[b]*ETH Zürich, 8092 Zürich, Switzerland*
[c]*Authors contributed equally to the work.*

Abstract

This paper provides a broad perspective and analysis of the work done in control of hybrid and convertible unmanned aerial vehicles (UAVs) for the main existing designs. These flying machines are capable of vertical take off and landing (VTOL) in *helicopter mode* and able to transition to high-speed forward flight in *airplane mode* and vice versa. This paper aims at helping engineers and researchers develop flight control systems for VTOL UAVs. To this end, a historical perspective first shows the technological advances in VTOL aircraft over the years. The main VTOL concepts and state-of-art flight control methods for VTOL UAVs are presented and discussed. This study shows both the common parts and the fundamental differences in the modeling, guidance, control, and control allocation for each hybrid-VTOL-UAV type. The open challenges and the current trends in the field are highlighted. These are namely: 1) augmenting or replacing classical controllers with data-driven methods such as neural networks and machine-learning-based controllers; 2) incorporating as much knowledge of the vehicle as possible into the flight controller, for example through model predictive control or model-based nonlinear controllers; 3) a trend towards finding a unified-control approach valid in all flight modes without the need to switch among flight controllers or to perform predefined-gain scheduling, and 4) the need to mitigate control complexity and available computing resources.

Keywords:
VTOL-flight transition control, hybrid and convertible aircraft, unmanned aerial vehicles (UAV), control allocation

1. Introduction

About a decade ago, unmanned aerial vehicles (UAVs) or flying drones were still mostly curiosities within some laboratories and still at early operational stages in the military and civil domains. In the last few years, there has been an enormous research interest for these flying vehicles, which have become very accessible to the public domain for a whole lot of commercial and industrial applications. These applications range from mapping, inspection, surveillance, search and rescue, forest-fire detection and monitoring, to name just a few. Recent advances in electric propulsion systems, high-storage batteries and modern control techniques have also opened up new possibilities for autonomous payload transportation and urban air-taxi mobility [1].

Aerial platforms can generally be separated into two categories, namely a) vertical take off and landing (VTOL) or rotary-wing (RW), such as helicopters and multirotor platforms, and b) fixed-wing (FW) aircraft. Depending on the application, each type has different advantages over the other. While VTOL UAVs do not require runways and have hover capabilities, they usually have a lower range than their FW counterparts and can generally carry smaller payloads. As summarized in Fig. 1, they are fundamentally different in their dynamics, aerodynamics and actuation, and therefore, different in the way they operate. However, RW and FW vehicles also present similarities, since they are both subject to four forces: gravity $\boldsymbol{F}_g$, drag force $\boldsymbol{F}_D$ opposite to the velocity vector $\boldsymbol{v}_a$, thrust force $\boldsymbol{T}$, and lift force $\boldsymbol{F}_L$.

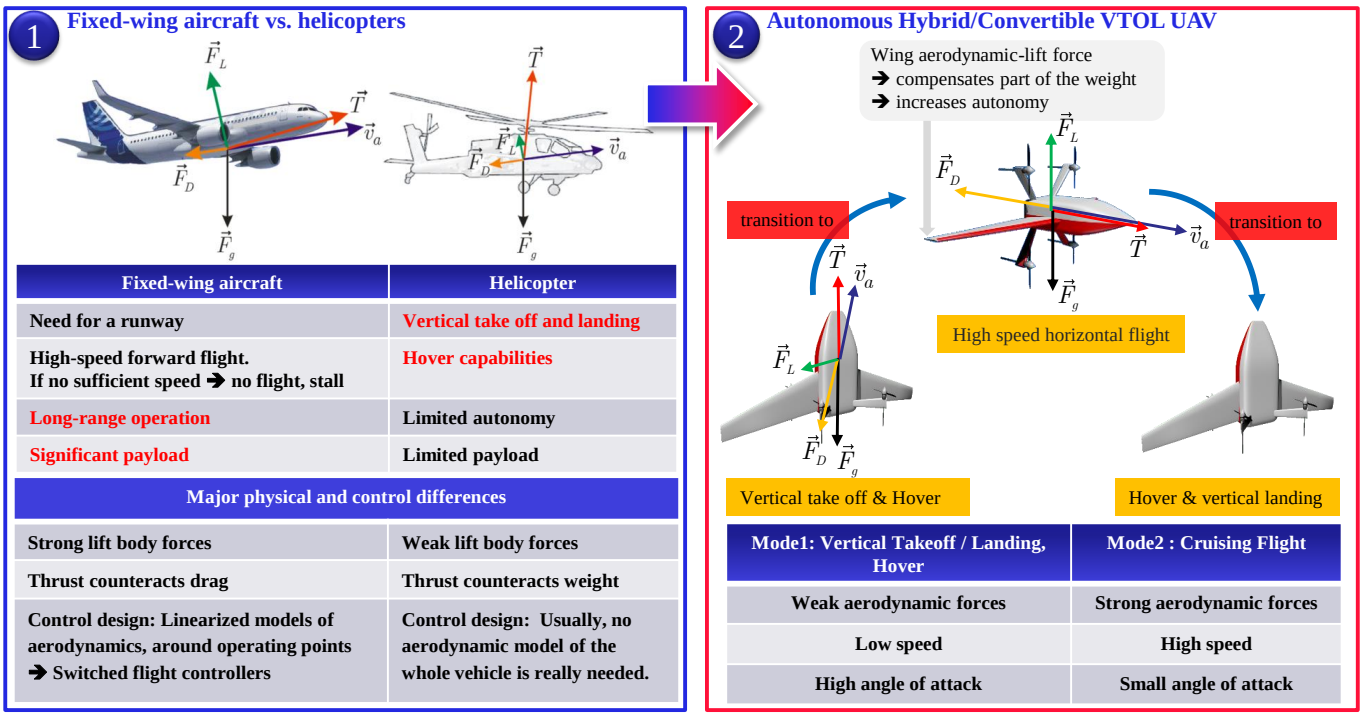

Figure 1: Fixed-wing aircraft vs. helicopter vs. a possible hybrid-VTOL aircraft: main properties. The respective advantages of fixed-wing aircraft and helicopters are highlighted in red.

As indicated in the bottom tables in Fig. 1, hybrid flying machines were developed with the intention to combine the benefits of both FW and RW vehicles, namely VTOL and hover capacity, superior flight maneuverability, increased payload capability, larger range of operation. This is done by tilting the rotors, the wings or even the entire airframe (see Fig. 1), to cruise efficiently at high speeds and to take off and land like a helicopter. However, the tilting motion results in highly-nonlinear dynamics and complex aerodynamic

effects, which complicates the trajectory generation and control of these vehicles. Further challenges come from the fact they have to operate in flight modes, in which the aircraft's behavior and dynamics are drastically different depending on the operating point or mode of operation. The flight control system should be valid over a large flight envelop, and in the presence of severe external perturbations, model uncertainties, possible actuator/sensor failure, taking into account actuator saturation and the possible under-actuated nature of such platforms.

The main goal of this paper is to provide an overview and comparison of the control methods used in hybrid UAV control and show how they are applied to the different platforms. Particular attention is paid to prototypes whose specifics (control structure, avionics, etc.) are available publicly, thus allowing meaningful comparison and analysis. As such, this work mainly focuses on convertible UAV designs and control techniques encountered in the scientific literature over the last twenty years.

Section 2 overviews and evaluates the major hybrid-VTOL vehicle designs with respect to mechanical complexity, stabilility concerns, efficiency and maneuverability. The primary focus is on research platforms. In order to provide some historical perspective, a selection of the most-prominent military or commercial projects, together with some prototypes, is also included for completeness. Section 3 reviews the physical modeling of the different hybrid-VTOL UAVs types and highlights fundamental differences and similarities. Next, a detailed review about feasible state-trajectory generation, vehicle control and control allocation is provided in Sections 4, 5 and 6, respectively. In this context, Section 5.3 includes a simulation-based comparison between two representative state-of-the-art control approaches. The paper concludes in Section 7 with an outlook on the still-open challenges in the field.

2. Platform Designs

While unmanned flying hybrid vehicles are a topic of modern research, several prototypes have already been developed to meet the needs of specific real-world applications. Section 2.1 provides a short historical perspective of such vehicles encountered in commercial, military and general non-research areas, whose specifics such as the type of avionics and control structures have not been found because of confidentiality. Thus, the remainder of this review focuses on convertible UAVs whose development process is documented in scientific publications. The considered vehicles are introduced in Section 2.2.

Table 1: A chronological selection of manned hybrid/convertible aircraft developments, each with a different VTOL configuration (non-exhaustive list).

Aircraft Type	Description	Comments
Lockheed XFV-1 [2, 3] 	• Official first flight: 16 June 1954. • The aircraft made a total of 32 flights. • Number of units produced: 1 flying, 1 incomplete • No vertical takeoffs or landings were performed. • The XFV-1 was able to make a few transitions after hover at high altitude. • The project was cancelled in June 1955.	• The pilot had very poor or no visibility of the ground during vertical takeoff and landing phases, making these maneuvers extremely difficult and dangerous to perform. • Only highly-experienced pilots could fly the aircraft.
NASA Vertol-Z2 [4, 5] 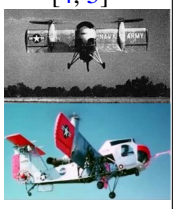	• Research aircraft built in the US in 1957. • Goal: testing wing-tilt approach to vertical take-off and landing. • The T-tail incorporated small ducted fans to act as thrusters for greater control at low speeds. • Number of units produced: 1 • In 8 years of development, only 34 transitions from VTOL to cruise were reported successful for a total of 450 flights. • Program stopped in 1965.	• Range of operation limited to 250 km. • Rather slow forward-motion speed of max 340 km/h. • Convertible capability demonstrated but remained very limited.
Hawker P1127 / Harrier [6, 7] 	• Aircraft equipped with a single turbine with several controlled nozzles deflecting the airflow downwards for the VTOL mode. • Aircraft design : Hawker Sideley/ McDonnell Douglas, GB/USA • First combat jet aircraft with VTOL capacity • Maiden flight in 1960. Retired in 2011 from Royal Air Force. • Other nations are still using it.	• Not capable of agile maneuvers, very slow motion at takeoff and landing. • The fully-equipped aircraft was too heavy to really perform VTOL. Rather used for short distance take-off and landing (STOL).
Curtiss-Wright X-19 [1] 	• First flight in November 1963. • VTOL capability thanks to four-tilting propellers of 4m diameter. • Program cancelled after the crash of the first prototype in August 25 1965.	• Maximum horizontal flight of 730km/h. • Payload of 500 kg.
Mirage IIIV [8, 9] 	• French airplane from Dassault Aviation equipped with 9 engines. • First flight in 1965, first successful transition from hover to high speed forward flight on March 24th, 1966. However, the Mirage was never able to take-off vertically and to successfully go supersonic in the same flight. • Program stopped in November 1966 after the crash of the second prototype.	• Expensive development. • Reported to be highly complex and dangerous to fly.
Bell X-22 [10, 1] 	• V/STOL experimental aircraft made of four tiltable ducted fans and four fixed forward turbines. • First flight in March 17, 1966. • Total 272 flights, 130 VTOL starts, 236 VTOL landings. • End of service in 1988.	• Considered at that time to be the best in class VTOL aircraft. • A failure in one of the fan-tilting mechanism caused the vehicle to crash.
Bell-Boeing V-22 [10, 11] 	• First flight took place in 1989 with successful transition only six months later. • Aircraft approved for serial production in 1997. • Highly sensitive to vortex ring state due to construction.	• Multiple fatal crashes during development process. • Reported to be very expensive in support and maintenance. • Slow transition maneuver (≈12 s).
F35-B SVTOL [12, 13] 	• US airplane from Lockheed Martin. • Compared to the A variant, the F35-B is similar in size but sacrifices about a third of fuel volume to accommodate the vertical flight system. • VTOL demonstration since 2011. • Lockheed Martin Vice President S. O'Bryan said that: "Most F-35B landings will be conventional to reduce stress on vertical lift components". • Lt. Gen. R. Schmidle said that the vertical lift components would only be used "a small percentage of the time" to transfer the aircraft from carriers to land bases.	• VTOL maneuver is very slow, inefficient and hardly possible with payload. • Aircraft is not as reliable as other versions of F35. • VTOL capabilities result in very heavy and expensive aircraft.

Table 2: A chronological selection of unmanned hybrid aircraft developments (non-exhaustive list)

Aircraft Type	Description and comments
Boeing Heliwing [14] 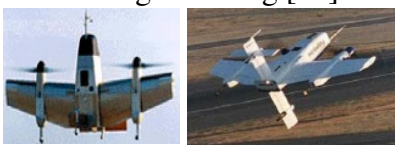	• Constructed by Boeing. • First flight in 1995. • Program cancelled after a crash two months later.
Panther [15] 	• Prototype from Israel where two front propellers can tilt. • Propeller at back is used only for VTOL phases. • Quite slow transition, sensitive to wind. • Not very agile.
Aurora Excalibur [16] 	• Aurora Excalibur: designed by Aurora Flight Science 2005 - 2010. • Two fixed ducted fan housed in the wing and one tilting turbine. • The available reports are not clear about the performance and transition capabilities.
Boeing Phantom Swift X-Plane Concept [17] 	• VTOL aircraft made of two fixed propellers embedded within the fuselage and two-tiltable ducted propellers located at each wing tip. • Selected for DARPA X-Plane competition in 2014 • Scale model only.
AgustaWestland Project Zero [18] 	• Developed by AgustaWestland as an all-electric vehicle. • Flight testing performed on small-scale models on June 2011. • Low flight duration due to limited battery, investigations currently carried out to increase autonomy. • Still under development.
Aurora XV24 LightningStrike [19] 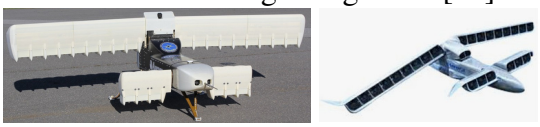	• Winner of the DARPA VTOL X-plane competition in 2016. • First successful flights in March 2017. • First tilt-wing UAV powered by an Electric Distributed Propulsion (EDP) system. • Twenty four variable-pitch ducted fans driven by electric motors provide thrust for both hover and cruise.
Wingcopter [20] 	• Produced by Wingcopter in Germany since 2014. • Propellers pivot for VTOL and forward cruise flight. • Holds Guinness World Speed record for highest cruise velocity in its category. • Successfully completed real-world medicine delivery tasks.
WingtraOne [21] 	• Produced by Wingtra in Switzerland since 2016. • Fully autonomous for take-off, transition and landing. • Successfully completed high-precision real-world aerial survey and mapping tasks.
Airbus Vahana [22] 	• Produced by Airbus Commercial Aircraft. First flight Jan. 31, 2018. • Tilting wing technology. Total of eight propellers. Max speed: 220km/h. • Project ended on February 2020.

2.1. Non Academic Research Applications

This section introduces a representative but non-exhaustive list of hybrid vehicles in a chronological order.

2.1.1. Most-known Manned Convertible Aircraft

Table 1 lists a non-exhaustive collection of manned vertical/short take off and landing (V/STOL) aircraft since the 1960s'. The interested reader is referred to [23, 24, 25, 26] for more complete reviews about manned V/STOL design concepts and their handling qualities, which were already defined as far back as the 1970s' [27]. As can be seen in Table 1, almost all the manned VTOL aircraft developed until recently were for military purposes only. Despite many attempts from the major fighter-aircraft constructors, only a few aircraft are really VTOL capable. These aircraft all display the same limited performance in agility, fuel-efficiency, autonomy and most importantly reliability. As of today, the Boeing-Bell V-22 Osprey aircraft is probably the most prominent human-piloted hybrid air vehicle, after the many deadly crashes it had during its development phase [10] and some following operations [28].

2.1.2. Known Projects about Unmanned Convertible Aircraft

Table 2 highlights developments of UAVs with VTOL capability and meant to transition to forward-cruising flight and vice versa. Only few projects have completed the initial development and testing phase, and even fewer projects have resulted in a fully operational full-scale vehicle. There are very few satisfactory convertible flying platforms capable of daily routine in the midst of civilian infrastructure with robust and safe operation.

2.2. Academic Research-project Prototypes

Table 3 provides an overview of the most common hybrid UAVs found in modern scientific literature within academic research. Three main types of unmanned VTOL platform are standing out, namely tailsitter-, tiltrotor-, and tiltwing-VTOL aircraft. A general comparison of the three regarding mechanical complexity, stability concerns, efficiency and maneuverability is provided in Table 4. Additional performance comparisons and evaluations for hybrid VTOL aircraft can be found in [26].

2.2.1. Tailsitter Aircraft

As the name suggests, tailsitters take off and land vertically on their tail. Since the rotors are usually rigidly attached to the aircraft, the entire airframe tilts forward to achieve horizontal flight. This flight-mode transition is done using aerodynamic-control surfaces or differential-rotor thrust only [77, 79]. Hereby, the former methodology is generally more efficient in cruise flight as it requires fewer propellers but it is also more complex to control compared to pure differential-rotor thrust. In any case, tailsitters are usually mechanically rather simple and light-weight, as they do not need any specific actuators for flight-mode transitions. However, the large exposed surface area of the fuselage and wing makes tailsitter UAVs less maneuverable and more prone to wind disturbances, especially during take off and landing [176]. Thus, hover efficiency is reduced, since more power is required to stabilize the system. Additionally, tailsitters experience high angle of attack (AoA) during low-speed operation, which makes the modelling and control more demanding. Fig. 2 provides examples of some tailsitter aircraft.

2.2.2. Tiltrotor Aircraft

Tiltrotor vehicles belong to the group of *convertiplanes*. Unlike tailsitters, the longitudinal body axis of these aircraft does not rotate much during the whole flight. Instead, a tilting mechanism is added to the

Table 3: Overview of academic-research hybrid UAV prototypes found in literature

Type	# Rotors	Remarks	Sources
Tailsitter	1	wing-fuselage design with primary control surfaces	[29, 30, 31, 32, 33, 34, 35, 36, 37, 38]
	1	ducted fan with control vanes	[39, 40, 41, 42, 43, 44, 45]
	2	flying-wing design with elevons	[46, 47, 48, 49, 50, 51, 52, 53, 54, 55, 56, 57, 58, 59, 60, 61, 62, 63]
	2	wing-fuselage design with primary control surfaces	[64, 65, 66, 67, 68, 69, 70, 71]
	4	flying-wing design with elevons	[72, 73, 74, 75]
	4	flying-wing design without control surfaces	[76, 77, 78, 79, 80, 81, 82, 83, 84, 85, 86, 87, 88, 89, 90]
	6	wing-fuselage design with primary control surfaces	[91, 92, 93, 94, 95]
Tiltrotor	2	rotors mounted on wings	[96, 97, 98, 99, 100, 101, 102, 103, 104, 105, 106, 107, 108, 109, 110, 111, 112]
	3	two rotors mounted on wings, one fixed tail rotor	[113, 114, 115, 116, 117, 118, 119, 120, 121, 122, 123, 124, 125]
	3	two rotors mounted on wings, one tiltable tail rotor	[126, 127, 128, 129, 130]
	4	rotors mounted symmetrically around center of gravity	[131, 132, 133, 134, 135, 136, 137, 138, 139, 140, 141, 142, 143, 144, 145, 146, 147, 148, 149, 150]
Tiltwing	3	two rotors mounted on wings, one tail propeller	[151, 152, 153, 154, 155, 156]
	4	two sets of wings at front and back	[157, 158, 159, 160, 161, 162, 163, 164, 165, 166, 167, 168, 169, 170, 171]
	5	four rotors mounted on wings, one tail propeller	[172, 173, 174, 175]

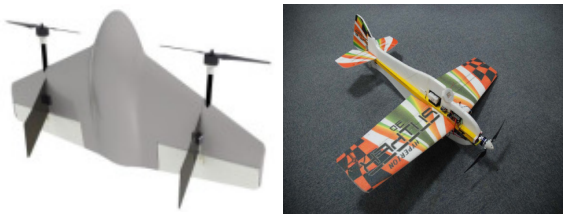

(a) Left: Flying-wing design [57]. Right: Wing-fuselage design [35].

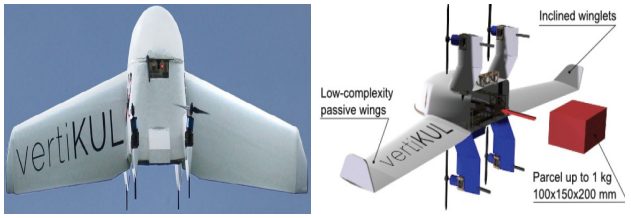

(b) Tailsitter with differential thrust only, no flaps [77, 79]

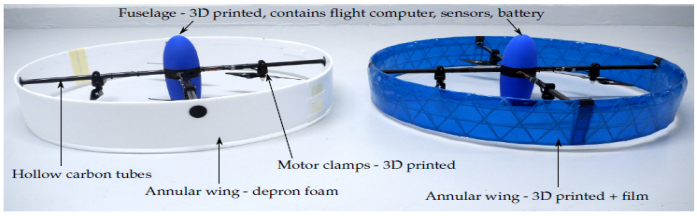

(c) Annular-wing fuselage design [85]

Figure 2: Examples of tailsitter UAVs

rotors for flight-mode transition. This way, the thrust direction can be rotated up for VTOL mode and be rotated forward for horizontal acceleration [176]. A two- and four-rotor design are shown in Fig. 3. A major disadvantage of the first implementation is the negative lift or download due to part of the wing being in the propeller wash. An in-depth analysis of these so-called *aerodynamic interference effects* and how they influence flight performance and stability is provided in [177]. On top of that, since this form of propeller mounting requires shorter and thicker wings, cruise flight efficiency is also reduced. At the cost of increased mechanical complexity, four rotor variants balance some of these disadvantages, although cruise flight is still inefficient due to the increased number of propellers. At low-speeds however, tiltrotor aircraft benefit from their multicopter-like construction and demonstrate high maneuverability and agility [178]. For example, large yaw torques can be produced by differentially tilting the left- and right- propellers [146, 147].

(a) Two-rotor design [105]

(b) Four-rotor design [75]

Figure 3: Examples of tiltrotor UAVs

2.2.3. *Tiltwing Aircraft*

In tiltwing aircraft, the rotors are rigidly attached to the wings and the entire wing rotates, while the fuselage mostly remains horizontal during flight. Similar to tiltrotor UAVs, the wing-tilting capabilities are achieved through the addition of dedicated actuators, which increases the mechanical complexity of the platform and might introduce actuation delays in the system. Because the propellers and wings move together, control surfaces on the wings (ailerons, flaperons) can still be used during hover due to the airflow generated by the propellers' downwash. Similarly to tailsitters however, the large exposed surface area of the wing during take off and landing increases the sensitivity to wind [176] and power consumption during hover, as well as limiting maneuverability. Regarding cruise efficiency, the fixed position of the propellers with respect to the wing allows to optimize the design of the latter and in turn its aerodynamic performance. Fig. 4 shows examples of designs with three and four rotors, respectively.

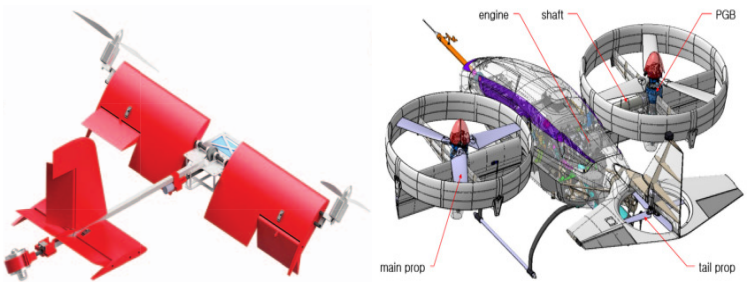

(a) Three-rotor design [152, 123]

(b) Four-rotor design [159]

Figure 4: Examples of tiltwing UAVs

Table 4: Performance comparison of different hybrid UAV platforms

	Tailsitter	Tiltrotor	Tiltwing
Mechanical Complexity	• Simple mechanical design • No dead-weight	• Complex propeller-tilting mechanism • Dead-weight of tilting actuators	• Complex wing-tilting mechanism • Dead-weight of tilting actuators
Stability Concerns	• Wind susceptibility during hover • High angle-of-attack operation	• Tilt-actuation delays • Aerodynamic interference effects	• Wind susceptibility during hover • High angle-of-attack operation • Tilt-actuation delays
Efficiency	• Power intensive disturbance rejection during hover • Efficient cruise through optimizable wing design	• Download reduces hover lift generation • Sturdy wing design reduces cruise efficiency	• Power intensive disturbance rejection during hover • Efficient cruise through optimizable wing design
Maneuverability	• Agility reduction from large wing drag	• Agile maneuvering through thrust-vectoring	• Agility reduction from large wing drag

3. Modeling of Hybrid/Convertible Aerial Vehicles

Proper modeling is essential for simulation and control of hybrid aerial vehicles. As described in Section 2, convertible UAVs combine :

- an actuation necessary for the vertical take-off and landing maneuvers, inspired by (multi-rotor) helicopters or thrust vectoring in VTOL jets,
- and an airframe that has some sort of wing, capable of generating aerodynamic lift forces at sufficient forward speed.

There is a significant body of literature describing the individual modeling of single- [179, 180] and multi-rotor helicopters [181, 182], as well as modeling of FW aircraft [183, 184, 185, 186, 187, 188], to name just a few. These models are mostly analytical and derived from first principles such as Newton's law, but could also be built from experimental data. This is particularly the case for the vehicle's aerodynamics, which are often studied via wind-tunnel experiments. However, most of the papers and text books present (almost) linear aerodynamical models, or nonlinear models but confined to quite restricted operating conditions (small AoA, low or constant speed). This is insufficient when it comes to modeling hybrid UAVs, which require the consideration of dynamic effects associated with high AoA conditions, as well as tilting propellers and wings.

In the case of tailsitters and tilt-wing aircraft, the aerodynamic model needs to be valid in the transition phases. This requires the extension of classical FW aerodynamics to high AoA and low speed operation [189]. In this regard, the comprehensive textbook of flight dynamics and aerodynamics by Stengel [185] and the work reported in [189] are helpful as they provide plots and discussions about such flight regimes. Additionally, the effect of propeller wash on the airfoils of the vehicle must be understood and considered in the system model.

On the example of a tiltwing UAV, the work in [155] identifies such areas of propeller-wing interaction and clearly separates their force-torque generation from the rest of the airfoil.

As mentioned in Section 2, propeller-wing interaction is also an important phenomenon in tiltrotor aircraft [177]. Wing download and similar aerodynamic effects related to propeller-induced airstream for tiltrotor UAVs are well documented and modeled in [190], based on momentum theory. Another approach using a lumped vortex model is shown in [191]. Continuous nonlinear functions to describe the aerodynamic lift and drag coefficients over the whole range of AoA for tiltrotor platforms are derived in [134]. Apart from the aerodynamics, gyroscopic effects due to the rotation of the propellers are also be considered, since they not only affect the thrust generation but also introduce counter torques on the vehicle.

As summarized in Table 3, there are many possible designs for a hybrid VTOL UAV. Although all models have common structure, there are major differences in the actual formulation of the force and torque terms mentioned above. These depend on the arrangement of the thrusters or propellers, the existence of aerodynamic control surfaces or not, and the shape of the vehicle. However, the detailed derivation of a customized modeling for a specific platform is out of the scope of this review. Instead, Section 3.1 shortly summarizes the equations common to all hybrid VTOL aircraft and then highlights the terms which need to be adapted depending on the flying platform at hand. Simplified examples for these expressions are then provided in Section 3.2 for tailsitter, tiltrotor and tiltwing UAV respectively to highlight fundamental differences and similarities among them. Hereby, the presented equations are purposely formulated fairly general and abstract to simplify the comparison. For a more detailed study, the interested reader is referred to the works mentioned above.

3.1. Common 6 Degree-of-Freedom (DoF) Translational and Rotational Dynamics

Let an inertial frame be denoted by $\mathcal{I} = \{\mathbf{0}; \boldsymbol{x}_I, \boldsymbol{y}_I, \boldsymbol{z}_I\}$ with $\boldsymbol{z}_I$ pointing downward to be consistent with the common use in aeronautics of the North-East-Down (NED) frames. The body frame is denoted $\mathcal{B} = \{\boldsymbol{G}; \boldsymbol{x}_b, \boldsymbol{y}_b, \boldsymbol{z}_b\}$, with the vehicle's center of mass $\boldsymbol{G}$. The orientation and angular rate of the aircraft body-fixed frame $\mathcal{B}$ with respect to the inertial frame $\mathcal{I}$ can be represented by an attitude quaternion $\boldsymbol{q}_{\mathcal{I}}^{\mathcal{B}} = \begin{pmatrix} q_0 & \boldsymbol{q}_v^\top \end{pmatrix}^\top \in \mathbb{H}$ where $\mathbb{H}$ is the Hamilton space and the body-rotation rates vector $\boldsymbol{\omega} := \boldsymbol{\omega}_{\mathcal{B}/\mathcal{I}}^{\mathcal{B}} = [p, q, r]^\top \in \mathbb{R}^3$. The corresponding rotation matrix $\boldsymbol{R}_{\mathcal{I}}^{\mathcal{B}}$ is obtained using the Rodrigues' rotation formula:

$$\boldsymbol{R}_{\mathcal{I}}^{\mathcal{B}} = \boldsymbol{I}_3 + 2q_0\boldsymbol{q}_{v\times} + 2(\boldsymbol{q}_{v\times})^2 \tag{1}$$

with 3×3-identity matrix $\boldsymbol{I}_3$, and the skew-symmetric matrix $(\cdot)_\times$ associated with the cross product, i.e. $\boldsymbol{u} \times \boldsymbol{v} = \boldsymbol{u}_\times \boldsymbol{v}$, $\forall \boldsymbol{u}, \boldsymbol{v} \in \mathbb{R}^3$. The position and velocity of the vehicle's center of mass $\boldsymbol{G}$ with respect to $\mathbf{0}$ are described by $\boldsymbol{p} \in \mathbb{R}^3$ and $\boldsymbol{v} \in \mathbb{R}^3$, respectively. Based on standard Newton-Euler equations, the general continuous-time 6DoF dynamics of hybrid UAVs then take the following form:

$$\dot{\boldsymbol{p}}^{\mathcal{B}} = \boldsymbol{v}^{\mathcal{B}} - \boldsymbol{\omega} \times \boldsymbol{p}^{\mathcal{B}} \tag{2}$$

$$\dot{\boldsymbol{v}}^{\mathcal{B}} = -\boldsymbol{\omega} \times \boldsymbol{v}^{\mathcal{B}} + g\boldsymbol{R}_{\mathcal{I}}^{\mathcal{B}\top}\boldsymbol{z}_I + \frac{1}{m}\left(\boldsymbol{F}_r^{\mathcal{B}} + \boldsymbol{F}_a^{\mathcal{B}}\right) \tag{3}$$

$$\dot{\boldsymbol{q}}_{\mathcal{I}}^{\mathcal{B}} = \frac{1}{2}\begin{pmatrix} 0 & -\boldsymbol{\omega}^\top \\ \boldsymbol{\omega} & -\boldsymbol{\omega}_\times \end{pmatrix}\boldsymbol{q}_{\mathcal{I}}^{\mathcal{B}} \tag{4}$$

$$\boldsymbol{I}^{\mathcal{B}}\dot{\boldsymbol{\omega}} = -\boldsymbol{\omega}_\times \boldsymbol{I}^{\mathcal{B}}\boldsymbol{\omega} + \boldsymbol{\Gamma}_r^{\mathcal{B}} + \boldsymbol{\Gamma}_a^{\mathcal{B}}, \tag{5}$$

with gravitational acceleration g, mass m and moment of inertia $\boldsymbol{I}^{\mathcal{B}}$. The total force and torque induced by the propellers/rotors/thrusters systems is denoted as $\boldsymbol{F}_r^{\mathcal{B}}$ and $\boldsymbol{\Gamma}_r^{\mathcal{B}}$, respectively. Similarly, $\boldsymbol{F}_a^{\mathcal{B}}$ and $\boldsymbol{\Gamma}_a^{\mathcal{B}}$ describe the

total aerodynamic forces and torques. As mentioned, the specifics of these four terms depend on the vehicle type. Simple examples to highlight the fundamental differences are shown in the next section.

3.2. *Vehicle-specific Modeling*

In order to customize the generic six DoF model presented in Section 3.1 to a specific hybrid VTOL UAV, it is necessary to adapt the vehicle's force and torque terms. Namely, they are:

- the propelling forces $\boldsymbol{F}_r^{\mathcal{B}}$ and the aerodynamic forces $\boldsymbol{F}_a^{\mathcal{B}}$ in (3) ,
- the torques due to propelling actuators $\boldsymbol{\Gamma}_r^{\mathcal{B}}$ and torques due to aerodynamics effects and control surfaces $\boldsymbol{\Gamma}_a^{\mathcal{B}}$ in (5) .

The following sections provide exemplary formulations of these expressions for each hybrid UAV type and offer a high-level comparison amongst them.

3.2.1. *Tailsitter Aircraft*

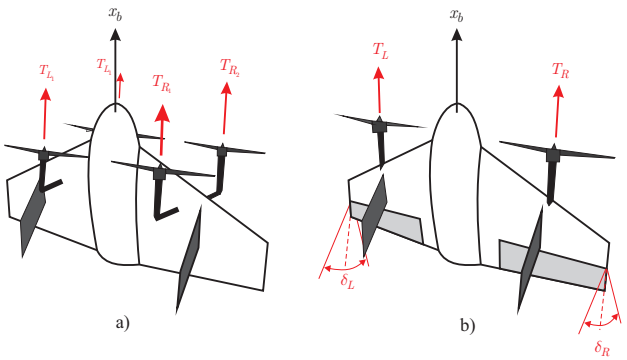

Figure 5: Tailsitter actuation. Case a): no control surfaces and four propellers. Case b) two propellers and two control surfaces.

Figure 5 shows two common configurations for a tailsitter VTOL aircraft. In case a) there are four propellers and no flap, in case b) there are only two propellers but two flaps are added. In both cases, the total propelling force vector $\boldsymbol{F}_r$ has a direction which is only along the longitudinal $x-$body axis $\boldsymbol{x}_{\mathcal{B}}$:

$$\text{case a):} \quad \boldsymbol{F}_r^{\mathcal{B}} = \begin{pmatrix} c_T\left(\omega_{L1}^2 + \omega_{L2}^2 + \omega_{R1}^2 + \omega_{R2}^2\right) \\ 0 \\ 0 \end{pmatrix} \qquad \text{case b):} \quad \boldsymbol{F}_r^{\mathcal{B}} = \begin{pmatrix} c_T\left(\omega_L^2 + \omega_R^2\right) \\ 0 \\ 0 \end{pmatrix} \tag{6}$$

with thrust coefficient c_T and rotor spinning rates ω_i. This means that the direction of $\boldsymbol{F}_r^{\mathcal{B}}$ is purely imposed by the vehicle orientation.

The aerodynamic force $\boldsymbol{F}_a^{\mathcal{B}}$ on the other hand depends on the air density ρ, the characteristic surface area S and the vehicle velocity $\boldsymbol{v}^{\mathcal{B}}$. In the absence of wind, it can be approximated as:

$$\boldsymbol{F}_a^{\mathcal{B}} = \frac{\rho}{2} S \left|\boldsymbol{v}^{\mathcal{B}}\right| \left(c_L(\boldsymbol{v}^{\mathcal{B}}) \boldsymbol{v}^{\perp \mathcal{B}} - c_D(\boldsymbol{v}^{\mathcal{B}}) \boldsymbol{v}^{\mathcal{B}}\right), \tag{7}$$

where $\boldsymbol{v}^{\perp \mathcal{B}}$ is orthogonal to $\boldsymbol{v}^{\mathcal{B}}$ and the airfoil span. Due to the construction of the tailsitter, the angle-of-attack and in turn the lift and drag coefficients c_L, c_D depend only on the body-frame velocity vector $\boldsymbol{v}^{\mathcal{B}}$.

To change the orientation of the vehicle, an appropriate torque needs to be produced, either through pure differential thrust (case a)) or through the combination of differential thrust and control surface deflections

(case b)). Hereby, the torque due to propelling actuators takes the form:

$$\text{case a):}\quad \boldsymbol{\Gamma}_r^{\mathcal{B}} = \begin{pmatrix} c_Q & -c_Q & c_Q & -c_Q \\ c_T l & -c_T l & c_T l & -c_T l \\ -c_T l & -c_T l & c_T l & c_T l \end{pmatrix} \begin{pmatrix} \omega_{L1}^2 \\ \omega_{L2}^2 \\ \omega_{R1}^2 \\ \omega_{R2}^2 \end{pmatrix} \qquad \text{case b):}\quad \boldsymbol{\Gamma}_r^{\mathcal{B}} = \begin{pmatrix} c_Q & -c_Q \\ 0 & 0 \\ -c_T l & c_T l \end{pmatrix} \begin{pmatrix} \omega_L^2 \\ \omega_R^2 \end{pmatrix}, \tag{8}$$

with torque coefficient c_Q and where l is the z- and y-axis distance from $\boldsymbol{G}$ to the rotors' center. Aerodynamic torques originating due to control surface deflections in case b) are obtained as follows:

$$\boldsymbol{\Gamma}_a^{\mathcal{B}} = \begin{pmatrix} c_F(\omega_R) & -c_F(\omega_L) \\ c_F(\omega_R) & c_F(\omega_L) \\ 0 & 0 \end{pmatrix} \begin{pmatrix} \delta_R \\ \delta_L \end{pmatrix}, \tag{9}$$

where the coefficient c_F captures the effectiveness of the control surfaces. Since they are located in the propeller down-wash, the effectiveness strongly depends on the corresponding rotor spinning rate. Although this complicates the actuator allocation, non-zero control authority is achieved even at hover.

3.2.2. Tiltrotor Aircraft

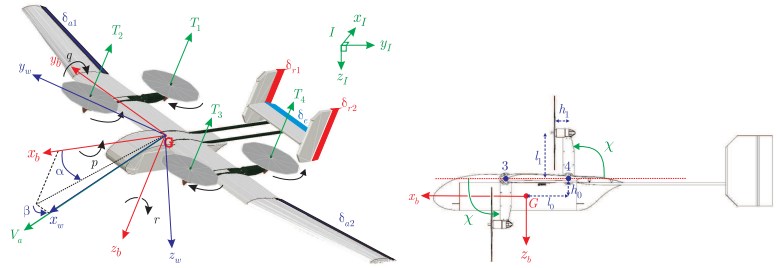

Figure 6: Left: tiltrotor in helicopter mode, propellers tilted by $\chi = 0$ [rad]. Right: fixed-wing mode, propellers tilted by $\chi = \frac{\pi}{2}$ [rad]. [134]

In the case of a tiltrotor aircraft, such as the one shown in Fig. 6, the total propelling force vector $\boldsymbol{F}_r^{\mathcal{B}}$ is not fixed in the body frame like with tailsitters (6) but rather depends on the tilting angle χ of the propellers:

$$\boldsymbol{F}_r^{\mathcal{B}} = \begin{pmatrix} \cos\chi & 0 & \sin\chi \\ 0 & 1 & 0 \\ -\sin\chi & 0 & \cos\chi \end{pmatrix} \begin{pmatrix} c_T\left(\omega_1^2 + \omega_2^2 + \omega_3^2 + \omega_4^2\right) \\ 0 \\ 0 \end{pmatrix}. \tag{10}$$

However, since the wing orientation is unaffected by the propeller tilting, aerodynamic forces $\boldsymbol{F}_a^{\mathcal{B}}$ are computed in the same fashion as for tailsitters (7):

$$\boldsymbol{F}_a^{\mathcal{B}} = \frac{\rho}{2} S \left|\boldsymbol{v}^{\mathcal{B}}\right| \left(c_L(\boldsymbol{v}^{\mathcal{B}})\boldsymbol{v}^{\perp\mathcal{B}} - c_D(\boldsymbol{v}^{\mathcal{B}})\boldsymbol{v}^{\mathcal{B}}\right), \tag{11}$$

Torque generation based on differential thrust is again different from tailsitters, as the orientation of the propeller forces relative to the body frame can change. To reflect this dependence on the tilt angle χ, equation (8) is augmented as follows:

$$\boldsymbol{\Gamma}_r^{\mathcal{B}} = \begin{pmatrix} \cos\chi & 0 & \sin\chi \\ 0 & 1 & 0 \\ -\sin\chi & 0 & \cos\chi \end{pmatrix} \begin{pmatrix} -c_T l & -c_T l & c_T l & c_T l \\ -c_T l & c_T l & c_T l & -c_T l \\ -c_Q & c_Q & -c_Q & c_Q \end{pmatrix} \begin{pmatrix} \omega_1^2 \\ \omega_2^2 \\ \omega_3^2 \\ \omega_4^2 \end{pmatrix}, \tag{12}$$

where l is the y-axis distance between $\boldsymbol{G}$ and the propellers' center, as well as the distance to the rotation axis. Depending on the specific construction of the tiltrotor vehicle, different types of aerodynamic surfaces are available. For the platform shown in Fig. 6, decoupled ailerons δ_A, elevators δ_E and rudders δ_R are present. As none of them is affected by propeller down-wash, the effectiveness c_F is only dependent on the body-frame velocity $\boldsymbol{v}^{\mathcal{B}}$:

$$\boldsymbol{\Gamma}_a^{\mathcal{B}} = \begin{pmatrix} c_F(\boldsymbol{v}^{\mathcal{B}}) & 0 & 0 \\ 0 & c_F(\boldsymbol{v}^{\mathcal{B}}) & 0 \\ 0 & 0 & c_F(\boldsymbol{v}^{\mathcal{B}}) \end{pmatrix} \begin{pmatrix} \delta_A \\ \delta_E \\ \delta_R \end{pmatrix}, \tag{13}$$

3.2.3. *Tiltwing Aircraft*

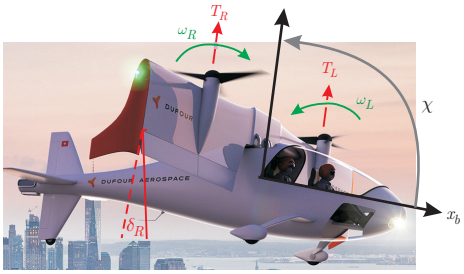

Figure 7: Tiltwing hybrid VTOL concept by Dufour Aerospace [192]

For a tiltwing aircraft, such as the one shown in Fig. 7, the propelling force $\boldsymbol{F}_r^{\mathcal{B}}$ has a direction which is a function of the wing-tilt angle χ, similar to tiltrotor aircraft (10):

$$\boldsymbol{F}_r^{\mathcal{B}} = \begin{pmatrix} \cos\chi & 0 & \sin\chi \\ 0 & 1 & 0 \\ -\sin\chi & 0 & \cos\chi \end{pmatrix} \begin{pmatrix} c_T\left(\omega_R^2 + \omega_L^2\right) \\ 0 \\ 0 \end{pmatrix}. \tag{14}$$

However, the wing-tilting capabilities makes the computation of aerodynamic forces more complex. The lift and drag coefficients no longer solely depend on the body-frame velocity vector $\boldsymbol{v}^{\mathcal{B}}$ as for tailsitters (7) and tiltrotors (11) but additionally change based on the current wing-tilt angle:

$$\boldsymbol{F}_a^{\mathcal{B}} = \frac{\rho}{2} S \left|\boldsymbol{v}^{\mathcal{B}}\right| \left(c_L(\boldsymbol{v}^{\mathcal{B}}, \chi)\boldsymbol{v}^{\perp\mathcal{B}} - c_D(\boldsymbol{v}^{\mathcal{B}}, \chi)\boldsymbol{v}^{\mathcal{B}}\right). \tag{15}$$

The current wing-tilt angle also affects differential thrust torque generation, same as for tiltrotor vehicles (12):

$$\boldsymbol{\Gamma}_r^{\mathcal{B}} = \begin{pmatrix} \cos\chi & 0 & \sin\chi \\ 0 & 1 & 0 \\ -\sin\chi & 0 & \cos\chi \end{pmatrix} \begin{pmatrix} -c_Q & c_Q \\ 0 & 0 \\ -c_T l & c_T l \end{pmatrix} \begin{pmatrix} \omega_R^2 \\ \omega_L^2 \end{pmatrix}, \tag{16}$$

with l being the y-axis distance between $\boldsymbol{G}$ and the center of the propellers. Aerodynamic surfaces on tiltwing UAV are often purposely placed in the propeller down-wash to maintain control authority and improve maneuverability at low velocities. This means that the effectiveness is primarily dependent on the rotor speed, as with tailsitters (9). However, as the propeller-wing assembly rotates with respect to the body, so does the generated aerodynamic torque:

$$\boldsymbol{\Gamma}_a^{\mathcal{B}} = \begin{pmatrix} \cos\chi & 0 & \sin\chi \\ 0 & 1 & 0 \\ -\sin\chi & 0 & \cos\chi \end{pmatrix} \begin{pmatrix} c_F(\omega_R) & -c_F(\omega_L) \\ c_F(\omega_R) & c_F(\omega_L) \\ 0 & 0 \end{pmatrix} \begin{pmatrix} \delta_R \\ \delta_L \end{pmatrix} \tag{17}$$

3.3. *Model Extension and Exploitation*

An accurate vehicle model is necessary for classical model-based control designs as shown in the next section, and especially for dynamic inversion or model predictive control approaches [98, 129, 143, 146]. Sometimes the modeling of the hybrid UAV is not accurate enough to enable satisfactory controlled behavior in both flight modes and transitions in between. In this case, online-adaptive control strategies, machine-learning approaches or neural-network-based controllers can be developed, as shown in detail in Section 5.

The insight gained from the modeling of the hybrid UAV can also be used for optimizing aircraft design as reported in [79, 193, 194, 195, 196, 197]. These works show how the flight performance and endurance are influenced by several key factors: take-off weight, power consumption, choice of battery, wing aerodynamic drag and lift, location of center of gravity, actuator number and arrangement [198], choice of propellers [199, 200, 201], etc. The authors of [197] conclude that VTOL-FW aircraft concepts which combine a fixed-wing airplane and the four propellers of a multirotor system have much less endurance than that of a FW concept only. While this is to be expected, they show how the design can be optimized to maximize endurance. The work reported in [202] proposes a modeling of the energy consumption of a class of small convertible UAVs. Propeller and wing modeling and the relative orientation between them during the transitions phases reveal the existence of energy-optimal configuration. The noise level can also be optimized as shown in [201]. This paper studies the aeroacoustic interactions between propellers and a tiltwing VTOL airframe. All the aforementioned key design aspects provide the necessary guidelines for the conception, the guidance and the control of convertible UAVs.

Finally, a rather accurate knowledge of the physical model of the UAV can be advantageously used to design actuator and sensor fault diagnosis systems and fault-tolerant flight controllers (FTC). Fault detection and isolation (FDI) systems compare the true dynamics of the aircraft, measured by sensors, with those predicted by a mathematical model, and thus assert the origin of behavior discrepancies. The interested reader desiring a comprehensive treatment of FDI systems and applications to FTC for aircraft may refer to [187, 203, 204, 205, 206]. An example of a fault-tolerant flight controller for a hybrid tailsitter UAV can be found in [60].

4. Analysis of State-trim and State-references for Flight-mode Transitions

As mentioned in Section 1, hybrid UAVs combine VTOL and hover capabilities with efficient forward-cruise flight. In order to fully exploit the advantages of the aircraft, the flight controllers must be able to perform a stable and efficient transition from *helicopter mode* to *airplane mode* and back. In both cases, the lift contributions from rotors and wings are combined during the transition maneuvers. Potential limitations in this combined lift generation (e.g. due to actuation constraints or wing construction) are the core factor that constrains the generation of appropriate transition trajectories. These constraints translate into the vehicle's state-space limitations in the form of a feasible flight envelope in which system's stabilization is possible. Thus, the controller development should be proceeded by assessing the steady-state flight envelope, i.e. the set of operating points for which a feasible dynamic equilibrium exists. This so-called *trim-point analysis* is not only used to generate state references for flight-mode transitions, but is also the basis for many common hybrid UAV control approaches (see Section 5.1) [207].

This section describes, how the feasible flight envelope of hybrid UAVs and appropriate operating points within it can be derived. As tailsitter UAVs change their attitude significantly during transition, while con-

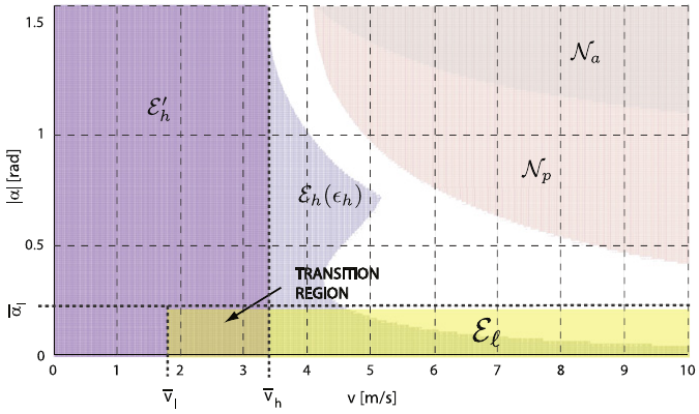

Figure 8: Tailsitter UAV flight envelope in the AoA-airspeed domain [208]

vertiplanes almost remain level, the corresponding analysis is addressed in separate ways for each vehicle type.

4.1. Tailsitter Aircraft

The authors of [208] identify a hover $\mathcal{E}'_h$ and level-flight $\mathcal{E}_l$ aerodynamic flight envelope within the airspeed (v) - AoA (α) domain, as displayed in Fig. 8. Hereby, $\mathcal{E}'_h$ describes the flight conditions where the aerodynamic forces are small compared to gravity forces. The level-flight envelope $\mathcal{E}_l$ is constrained by the stall speed of the aircraft $\bar{v}_l$ and an AoA $\bar{\alpha}_l$, where the relationship between the lift force and the AoA is mostly linear for $|\alpha| \leq \bar{\alpha}_l$. The intersection between the two areas $\mathcal{E}'_h$ and $\mathcal{E}_l$ defines the *transition region*, where both the hover and the level-flight approximations hold. As shown in Fig. 8, this *transition region* corresponds to a very small part of the possible flight regimes in the v-α domain. Therefore, the transition trajectory needs to be generated carefully. In addition, two low-controllability areas are detected. Specifically, the area $\mathcal{N}_p$ corresponds to flight conditions where aerodynamic drag exceeds maximum propeller thrust. The area $\mathcal{N}_a$ corresponds to flight regimes where the control surfaces have insufficient control authority to counteract torque disturbances. Once such a feasible flight envelope is found, [68, 41] show how a corresponding stable transition trajectory based on continuous velocity and pitch angle references can be derived. The works reported in [208, 50, 71] use an optimization algorithm to find suitable velocity and pitch angle references, where actuator constraints or low-controllability areas are explicitly taken into account. The evaluation of these reference functions at a desired number of points provides a set of trim flight conditions, which can then be used for trim point-based controller design (see Section 5.1.2). Examples of how to directly obtain discrete trim points from the model equations or from flight-test-based velocity-attitude maps are presented in [209] and [78], respectively.

To reduce the complexity associated with the derivation of the flight envelope and corresponding state references, some works simply command a step input in the pitch-angle reference to achieve flight-mode transition [64, 30, 31, 65, 76, 36, 56]. These methods are often combined with constant acceleration or altitude-hold controllers for the translational dynamics as shown in Fig. 9. However, the resulting reference trajectories are not always part of the feasible flight envelope. Thus, controllability and stability are not guaranteed with such a simple method. The same issue appears when using linear pitch-angle references [44, 77, 49, 87, 73, 88, 70, 72, 69, 84] instead of step inputs.

In most controllers (see Section 5.1), attitude reference values from the trim analysis will be treated as feed-forward terms and combined with references from thrust vector alignment. Due to their construction, the thrust direction of tailsitter vehicles is always aligned with the main body $x-$axis, according to equation (6). Therefore, the attitude references need to be chosen, such that the resulting thrust vector is aligned with the

desired force vector for translational tracking, just like with regular multicopters [210, 71]. In helicopter mode, this thrust vector alignment is often achieved by using a simple proportional guidance law [64, 40, 41] or by treating the attitude as a virtual input to the translational dynamics [62, 61, 31, 211, 187, 47, 81]. During high-velocity cruise, L1 guidance [212, 213, 71, 32] or similar radius-computation laws [64, 214, 41] are used to achieve a coordinated-turn without sideslip. Alternatively, nonlinear thrust-vector alignment functions are used in [37, 53, 57, 59], which allow for the generation of an attitude reference which is independent of the flight configuration. Similarly, global trajectory generation is achieved through optimization in [215, 80]. Due to the large changes in the pitch angle, a quaternion-based attitude representation is often chosen in the attitude controller, in order to compute a singularity-free and well-posed attitude error [66, 216].

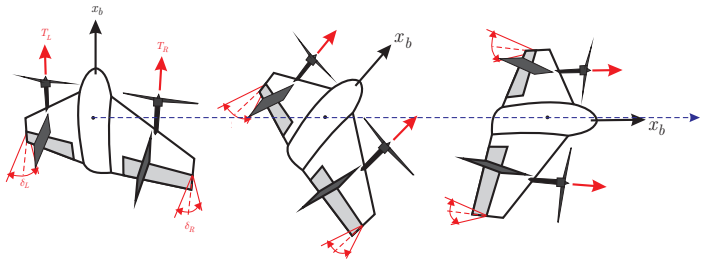

Figure 9: Transition maneuver of a tailsitter aircraft at constant altitude

4.2. Tiltrotor Aircraft

It is a common method to directly determine the possible operating range and flight envelope of tiltrotor UAVs based on the trim-point analysis [207]. For tiltrotor UAVs, stable flight conditions can be evaluated at trim-points scheduled in the *velocity − rotor-tilt angle domain* [217, 119] such as shown in Fig. 10. The resulting stability corridor is limited by actuator and lift-force generation constraints. Due to uncertainties in aerodynamic and motor parameters, operating the vehicle close to edges of the stable flight envelope should be avoided as indicated in [100, 120]. To make the transition process as stable as possible, the range of useful equilibrium points is often further restricted, by a constant pitch or flight-path angle constraint as shown in [100, 218, 131, 113, 133, 219, 137, 220, 141]. Regarding the AoA, the work in [219] schedules trim-points over the range of propeller-tilt angles and aims for optimal lift to drag ratio, while the work in [221] ensures that the AoA remains small and far away from the stall region.

The generation of feasible state references for flight-mode transition is usually based on the same trim-point analysis. For example, the transition trajectory can be generated based on rotor-tilt angle patterns apriori specified by the user. This method uses either a number of rotor-tilt-angle step inputs as in [130, 220, 122] or a linear reference for the rotor-tilt angle as in [104, 218] to schedule the trim-points. Depending on the desired rotor-tilt angle, the corresponding steady-state values are loaded and used as references in the controller. To avoid discontinuities in the references due to the finite number of trim-points, the authors of [222] and [109] fit a higher-order function, thereby creating a continuous and mostly smooth way to compute the steady-state values for any rotor-tilt angle. Another trajectory generation method relies on velocity inputs being provided by the user. Using the vehicle velocity as a scheduling variable, step [223, 219, 137] or linear [113, 140, 117, 141] references have been investigated. The desired values for the remaining state variables can then be obtained from trim-points, similar to the rotor-tilt-angle based methods.

Given enough trim-points, [102, 106] have shown that translational-velocity based methods are not limited to the transition phase but can also be used to generate stable trajectories for helicopter mode and cruise-flight mode as well.

In general, selection of an appropriate pitch angle reference during the transition process is not immediately intuitive. As shown in Fig. 11, the common method of initial acceleration through pitch-down in *helicopter-to-airplane* transition (like a regular multicopter aircraft) causes downward wing-lift forces, which is the opposite of the desired aerodynamic effect. To compensate the weight of the vehicle, the aircraft has to pitch up while tilting the propellers forward in a way that lift points upward, so that the propelling thrust progressively gets dedicated to the sole purpose of forward thrust.

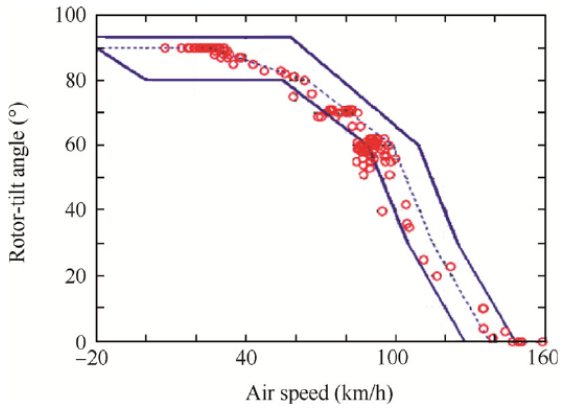

Figure 10: Tiltrotor UAV flight envelope. Rotor-tilt angle as a function of airspeed. [58, 144, 147]

Usually, only a small number of the computed trim-points are used as linearization points for the flight controllers (more details are in Section 5.1.3). Similar to tailsitter vehicles, state references from the trim analysis are then combined with references originating from thrust vector alignment. This alignment can be achieved through both attitude and tilt-angle changes, as shown in equation (10). However, it should be noted that the linearization based control approaches almost never modify the tilt-angle given by the trim analysis, i.e. thrust vectoring is purely done by changing the attitude.

Alternatively, the paper by [142] presents a completely trim-point-free approach, where the rotor-tilt angle and attitude reference are chosen such that the commanded thrust is minimized for a given position and velocity reference. Another approach is presented in [143, 146, 147], where an online Model Predictive Control (MPC) optimization algorithm, intrinsically taking into account actuator and aerodynamic constraints, also generates feasible attitude and tilt angle trajectories without trim points. The transition maneuver is obtained by simultaneously 1) minimizing the altitude change during the transition phase, and 2) by optimizing the vehicle pitch angle for wing-lift force generation during transition towards airplane mode or optimizing the wing-drag force for the transition towards helicopter mode. Similar ideas are also developed in [128, 136, 111].

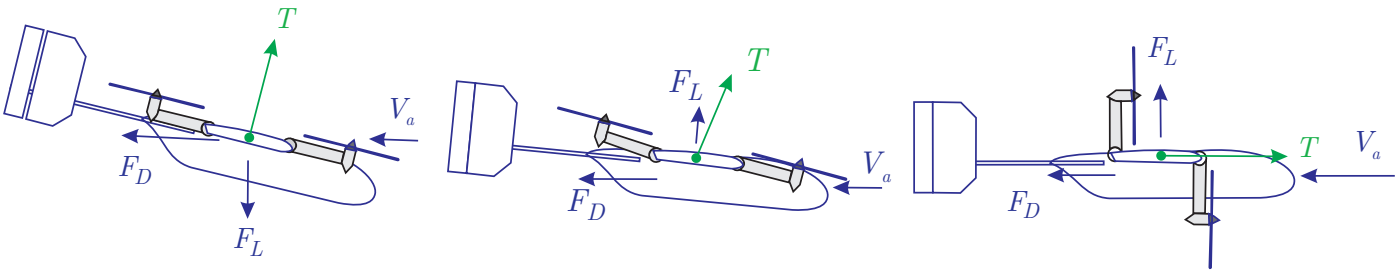

Figure 11: Tiltrotor transitioning from hover to cruise mode. The airspeed is V_a, the wing-lift force is F_L, the drag force is F_D, the propeller thrust is T.

4.3. Tiltwing Aircraft

Similarly to tiltrotor aircraft, the feasible flight states of tiltwing vehicles are often determined from a trim-point analysis. Hereby, trim-points are either scheduled by gridding the *velocity − wing-tilt angle* domain or the *velocity − pitch angle* domain [173, 151, 163, 171]. Due to the high-dimensional state space, the equilibrium points are not unique and allow the introduction of additional constraints or optimization criteria. For example, the algorithms presented in [174, 175, 153, 154] exploit the remaining DoF to enforce symmetric control inputs or to combine complementary control surfaces or to select more efficient steady-state solutions. Quite efficient flight conditions have also been obtained in [153, 154] by setting the trim pitch angle to zero at small velocities and equal to the flight-path angle at higher speeds. To achieve even better performance, the approach in [174, 175] formulates a separate optimization problem to find optimal pitch trim values within the flight envelope. In most papers, the transition trajectory is directly generated from the derived trim-points, similar to tiltrotor vehicles.

Once again, given a desired scheduling velocity and pitch angle, the corresponding steady-state control inputs, including wing-tilt angles, are used as feed-forward terms in trim-point based control approaches (see Section 5.1.4) [173, 163]. The overall attitude reference is then generated by combining steady-state values with a thrust-vector-alignment command. As for tiltrotor vehicles, the inherent overactuation allows to modify the thrust direction through either changing the vehicle attitude or the wing-tilt angle, as shown in equation (14) and Fig. 12. That being said, the tilt-angle reference given by the trim analysis is almost never modified. Instead, the required attitude references are computed from coordinated-turn requirements as shown in [174, 175, 151] or from objective optimization as in [154]. Other approaches make use of dynamic inversion and virtual control inputs [161, 160, 165, 166] to compute the necessary rotations.
Otherwise, trim-point free approaches allow for less restricted distribution between attitude and tilt-angle commands for thrust vector alignment. For example, the work presented in [167] employs a simple transition process by manually designing a linear wing-tilt angle reference, combined with dynamic inversion for attitude reference computation. [155] uses a nonlinear MPC implementation, similar to what was presented in [143, 146] for a tiltrotor vehicle, to obtain optimal thrust, attitude and wing-tilt angle commands.

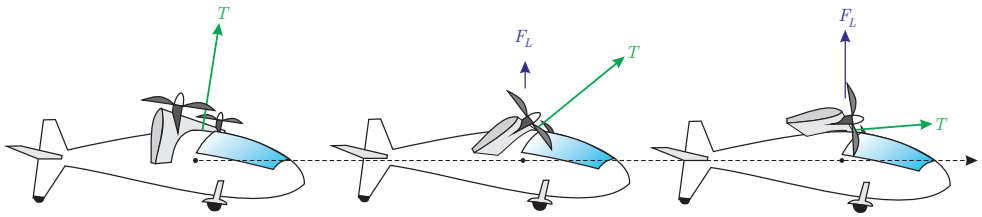

Figure 12: Tiltwing aircraft transitioning from hover to cruise mode. The airspeed is V_a, the wing-lift force is F_L, the drag force is F_D, the propeller thrust is T.

5. Control of Unmanned Hybrid/Convertible Aerial Vehicles

The automatic control of hybrid UAVs is still a challenge today, mainly due to the highly nonlinear dynamics resulting from the interaction of different aerodynamic effects (see Section 3). The transition maneuvers between helicopter and airplane modes, and vice versa, are particularly challenging as they require the flight controller to be able to handle potentially large changes in AoA (in particular for tailsitter aircraft), in velocity, in attitude and in actuator control effectiveness depending on airspeed, which all affect the aerodynamic forces and torques acting on the vehicle.

A major difficulty comes from the fact that classical methods to capture these aerodynamic characteristics, such as computational fluid dynamics (CFD) or wind tunnel measurements, do not provide analytical expressions. From a control design perspective, these methods are only useful to finely tune a controller around a given flight velocity. Thus, most control systems used in aeronautic and aerospace applications are based on linearized systems at certain operating points [184, 224], usually those of quasi-stationary flight for RW or equilibrium trajectories for FW aircraft.

The idea of having different controllers designed for specific operating conditions is a common approach in hybrid UAVs but requires the design of controller switching or scheduling policies as discussed in Section 5.1.

However, these methods are limited to specific areas of the flight envelope due to a finite number of linearization points and thus limit the domain of stability. In addition, small hybrid VTOL UAVs are particularly sensitive to wind perturbations, which existing autopilots, based on linear control techniques, cannot handle properly [176].

In order to circumvent these limitations and ensure stable tracking performance, more recent investigations propose the use of unified control approaches, based on adaptive or nonlinear implementations. These methodologies, capable of handling the nonlinear dynamics and covering the entire flight envelope, are discussed in Section 5.2.

It should be noted that literature focusing exclusively on hover or FW flight is not discussed in this section, since these works often employ standard control approaches from the RW or FW community. Instead, control methodologies which can be used across the full flight envelope of hybrid UAVs are introduced and compared.

5.1. *Scheduled Control Approaches*

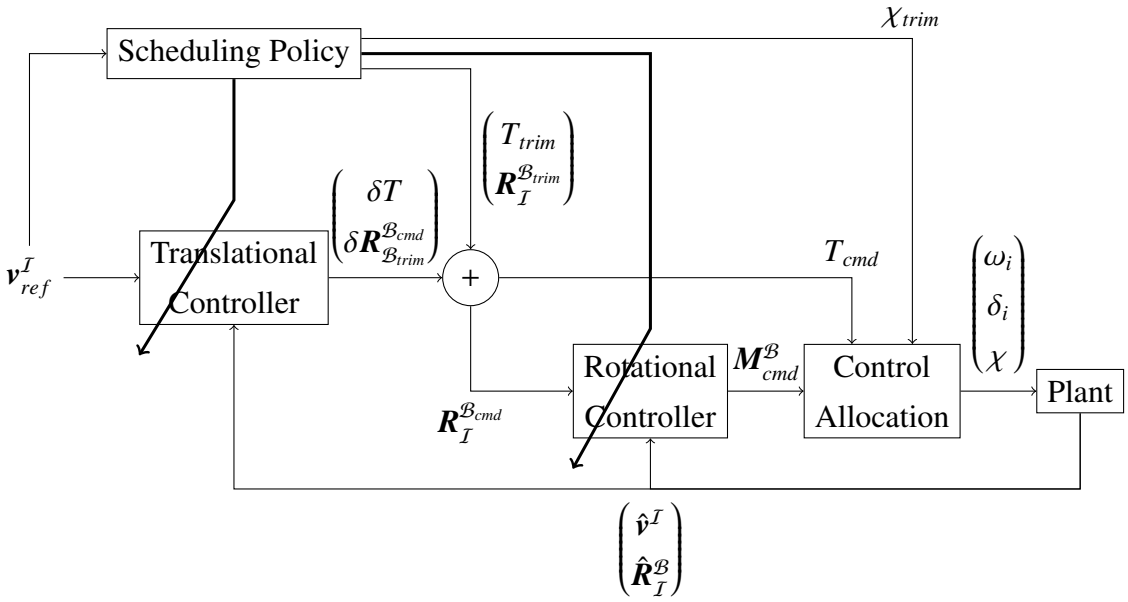

Figure 13: Scheduled control approach: Given a desired velocity reference $\boldsymbol{v}_{ref}^{\mathcal{I}}$, the scheduling policy loads the translational and rotational controller of the corresponding linearization point. The associated trim values for the thrust T_{trim} and attitude $\boldsymbol{R}_{\mathcal{I}}^{\mathcal{B}_{trim}}$ are then combined with the controller commands, namely the thrust δT and the thrust vector alignment attitude $\delta \boldsymbol{R}_{\mathcal{B}_{trim}}^{\mathcal{B}_{cmd}}$. Control torques $\boldsymbol{M}_{cmd}^{\mathcal{B}}$ from the rotational controller are fed into the control allocation, together with the total thrust T_{cmd} and the trim tilt angle χ_{trim} (only for tiltrotor and tiltwing vehicles) to compute the actuator commands for the hybrid UAV.

A promising concept for hybrid UAV control is to linearize the system around a finite set of trim-points (see Section 4) in the flight envelope and design a specifically tuned controller for each of them. In other

words, the flight envelope is discretized into a desired number of operating points and a single independent controller is developed for each one. As the current flight configuration changes, the appropriate control law needs to be loaded, which is done through so-called *controller-scheduling policies*. The general structure of scheduled control approaches is visualized and explained in Fig. 13. It should be noted that the tilt angle for tiltrotor and tiltwing hybrid UAVs is not modified by the controller itself but rather loaded from the trim-point analysis. In that sense, it is only computed offline without the possibility for online adaptation. While this simplifies the controller synthesis and allows for the use of standard RW and FW control laws and thrust vector alignment methodologies, it is also a major limitation of scheduled control approaches (see Section 5.3).

5.1.1. *Controller-scheduling Policies*

During flight, the current operating region of the system is captured by so-called scheduling variables and the corresponding control law, as well as the feed-forward terms of the respective trim point are loaded by the scheduling policy. The two most common implementations are shown in Fig. 14:

- The *Divide and Conquer* approach discretely switches between the different control laws, such that only one controller is running at a time.
- Contrarily to Divide and Conquer, *Control Authority Weighting* continuously fuses commands from two scheduled controller, based on a scheduling-variable dependent weight.

Tuning the individual controllers' dwell time to be smaller than the parameter-variation time constant generally results in good local performance. However, one needs to be careful regarding the global closed-loop stability and performance, as stated in [225].

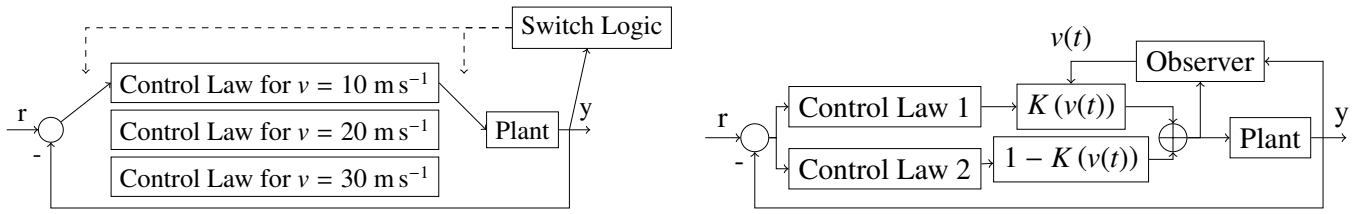

(a) Divide and conquer

(b) Control authority weighting

Figure 14: Common scheduling policies with the velocity $v(t)$ as and exemplary scheduling variable

5.1.2. *Tailsitter*

The method named as Divide and Conquer is used most often in tailsitter control, based on a well-tuned controller for each flight phase, namely hover, transition and cruise phases, respectively [67]. Sometimes, the transition controller is even omitted and one of the other two is used instead [32, 226]. On the other hand, [55] refines the controller grid, by using a larger number of trim points along the transition trajectory. In all cases, the correct controller is chosen depending on airspeed and pitch angle scheduling. Two scheduled controllers for VTOL and cruise modes are designed in [49] for Control Authority Weighting. During transition, they run simultaneously and the overall command is computed as:

$$u(\Delta t) = \left(1 - \frac{\Delta t}{T_T}\right) u_{VTOL}(\Delta t) + \frac{\Delta t}{T_T} u_{cruise}(\Delta t) \tag{18}$$

for the example of a transition between hover mode to cruise mode. Hereby, T_T is the transition duration parameter and Δt is the time since the beginning of the transition maneuver.

Regarding the control laws themselves, the most-commonly used one is P/PD/PID control, since it is intuitive to tune and only requires limited knowledge of the system. Nevertheless, PID control often performs very well and it is a great starting point for designing more advanced controllers. The general Proportional Integral Derivative (PID) control law takes the following form

$$u_{PID}(t) = K_P e(t) + K_I \int_0^t e(\tau)d\tau + K_D \frac{de(t)}{dt} \tag{19}$$

where the error vector is $e(t) = x_{ref}(t) - x(t)$ and where the gains K_P, K_I and K_D can be individually tuned to achieve the desired closed-loop system behaviour. As an example, the authors in [67, 68] select the gains to guarantee Lyapunov and input-to-state stability respectively. Controller augmentation through the use of trim maps is presented in [78].

Another frequent control law in tailsitter UAVs is Linear Quadratic Regulator (LQR), which optimizes the controller design for the linearized system of the form $\dot{x} = Ax + Bu$. The control input u is chosen as

$$u = -Kx. \tag{20}$$

Hereby, the gain matrix K optimizes the closed-loop system performance wrt. the cost function

$$J = \int_0^\infty x(\tau)^T Q x(\tau) + u(\tau)^T R u(\tau) d\tau, \tag{21}$$

where Q and R are the error and input weighting matrix, respectively. While the LQR controller generally has good robustness properties, optimality is no longer ensured if there are modeling errors and disturbances present in the system. A detailed discussion of this issue and corresponding comparison between model-free PID and model-based LQR control of a tailsitter is provided in [55].

5.1.3. Tiltrotor

It has been shown in Section 4.2 that the trajectory generation of tiltrotor UAVs is strongly based on trim states. Accordingly, most control structures are using the same trim points to employ Divide and Conquer methodologies. Using rotor-tilt angles or airspeed as scheduling variables, this approach has for example been investigated in [106, 220]. The work in [138] reduces the number of controller switches, by using only one controller per flight stage or even just two controllers for hover and cruise modes. Alternatively, Control Authority Weighting has been successfully applied in multiple different occasions. In [140], the controllers are weighted based on their underlying model, by evaluating the quality of the approximation at each iteration. Other applications use the reference tilt angles to distribute the control authority between VTOL and cruise controllers [130]. In [144], the airspeed is used to modify the relative weight between two velocity controllers running in parallel, one designed for RW and one for FW mode.

As for tailsitters, the P/PD/PID control law shown in equation (19) is a well established choice for tiltrotor UAV control in combination with the mentioned scheduling policies. LQR and general state feedback methods are also widely used. Here, the Bryson's rule is presented for a tiltrotor UAV as an example of a tuning method in [227], where the weights are the inverse of the respective maximum state- or input-allowed value squared. To reduce the design complexity and computational burden associated with having many isolated trim-points, [109, 228] used a robust Sliding Mode Control (SMC) that only requires two such linearization points instead. SMC is known to provide robustness and finite-time convergence to the controlled system [229]. However, one drawback of this approach is the chattering phenomenon of the control signal, caused by the *zig-zag*

motion of the state along the sliding surface. For a system with state $x = (\, x_1^\top \; x_2^\top \,)^\top$ where uncertainties only affect x_2, SMC defines a sliding surface

$$\sigma(x) = \begin{pmatrix} K & \mathbb{I} \end{pmatrix} \begin{pmatrix} x_1 \\ x_2 \end{pmatrix} = Lx. \tag{22}$$

The gain K is chosen such that it stabilizes the $\dot{x}_1$ subsystem. Trying to achieve $\sigma(x) = 0$, the control input u is designed to fulfill $\sigma(x)\dot{\sigma}(x) < 0$ by choosing

$$u = (LB)^{-1} \left(-LAx\right) - a \, \mathrm{sgn}(\sigma(x)) \tag{23}$$

where a is a tuning parameter. To avoid the common chattering phenomenon, [228] incorporates fuzzy control into the baseline SMC implementation.

5.1.4. Tiltwing

Just like with tiltrotor vehicles, tiltwing controllers rely on a set of trim points (see Section 4.3) in the flight envelope. Example designs using airspeed and wing-tilt angle as scheduling variables for the Divide and Conquer technique are shown in [154, 175]. Rather than using a large number of different controllers, the works in [151] and [165] only switch between three different control laws, namely one for VTOL, cruise and transition flight. In [156], a standard RW and FW controller are linearly mixed depending on the reference wing-tilt angle in a form of Control Authority Weighting. To ensure satisfactory flight performance during the transition despite these few trim points, a model-uncertainty compensation term computed by a Neural Network (NN) is added, somewhat similar to *Dynamic Inversion* (see Section 5.2).

P/PD/PID control laws as introduced in equation (19) are fairly common, where standard tuning methods are used to achieve stable and accurate tracking performance at each operating point. In addition, the work in [154] mentions how pitch-error dependent controller gains can be used to account for non-symmetric pitch authorities.

The second control law frequently encountered in scheduled control approaches for tiltwing aircraft is H_∞. According to the signals and systems depicted in Fig. 15, the goal is to minimize the effect of the worst possible disturbance w on the performance variable z through a feedback controller of the form $u = K(s)y$. In other words, K is chosen, such that $\|F(P, K)\|_\infty$ is minimized, where $F(P, K)$ is the transfer function from the disturbance w to the error signal z. While [171] uses a so-called μ-synthesis method to obtain the controller gain K, the research group at the Arizona State University [173, 174, 175] rely on mixed-sensitivity weighting functions. Compared to the standard μ-synthesis, this method allows to individually weight both the sensitivity and complementary sensitivity transfer functions.

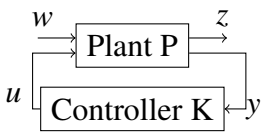

Figure 15: H_∞-control components

5.2. Unified Control Approaches

The scheduled control approaches presented in the previous section exhibit several shortcomings when it comes to hybrid UAV control. Since the number of linearization points considered in the scheduling policies

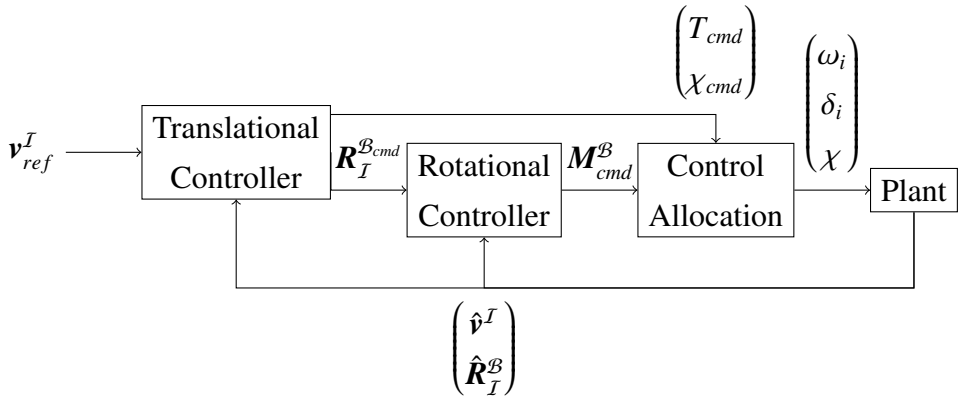

Figure 16: Unified C control approach: Given a desired velocity reference $\boldsymbol{v}_{ref}^{\mathcal{I}}$, the translational controller directly computes the total thrust command T_{cmd}, as well as tilt angle χ_{cmd} (only for tiltrotor and tiltwing vehicles) and attitude values $\boldsymbol{R}_{\mathcal{I}}^{\mathcal{B}_{cmd}}$ for thrust vector alignment. Control torques $\boldsymbol{M}_{cmd}^{\mathcal{B}}$ from the rotational controller are fed into the control allocation, together with the previously obtained total thrust and tilt angle commands to compute the actuator commands for the hybrid UAV.

is finite, the overall control structure is limited to specific areas of the flight envelope. Consequently, aerodynamic effects acting on the vehicle during transition can often not be considered adequately. Furthermore, the required controller switching might affect the stability, in case the scheduling parameter varies quickly with respect to the controller convergence. Finally, the restriction to use offline computed tilt angles from the trim map only for tiltrotor and tiltwing hybrid UAVs limits the capabilities of these vehicles.

Thus, a trend towards unified control approaches can be observed, whereby a single controller is deployed over the entire flight envelope. This concept is visualized and explained in Fig. 16. As shown, this methodology combines the tilt angle and attitude reference computation for thrust vector alignment in tiltrotor and tiltwing vehicles, unlike for scheduled control approaches. Although, novel strategies are required to distribute control authority between the two, the combined formulation allows for online optimization to improve flight performance and efficiency (see Section 4.2 and 4.3). Often, adaptive control methodologies are employed to handle the changing aerodynamic effects and control authorities.

5.2.1. Tailsitter

State-of-the-art literature on tailsitter UAV control shows several cases, where *Robust Control* with constant gains and without any additional compensation terms has been used successfully across the full flight envelope. Rather than adapting to system changes, aerodynamics and uncertainties, the idea here is to make the controller robust against them [207]. That being said, these works often require additional modifications in the control structure to achieve satisfactory performance. [56] and [76] use an external maneuver generator to obtain suitable attitude references, while [70] derived a custom mapping to account for the effects of forward and rotational speed on the propeller thrust, as well as using a special tuning function to ensure robustness. In [34, 78], it is explicitly mentioned that fixed gains in the controller are not optimal. This issue is addressed in [36] which demonstrates the use of *Direct Gain Scheduling*, whereby the controller gains are scaled with an airspeed $v(t)$ depending factor $k(v(t))$, i.e.:

$$k(v(t)) = \frac{v_{ref}}{v(t)} \tag{24}$$

where v_{ref} is a tuning parameter. The idea is to make the gains smaller, as the control surface become more effective at larger airspeed.

A simple solution to improve performance is to rely on *Dynamic Inversion*. This methodology allows to transform a nonlinear system such that it can be controlled as if it were linear. Given a nonlinear system of

the form

$$\dot{x} = f(x) + g(x)u, \tag{25}$$

the control input is designed as

$$u = g(x)^{-1}\left(-f(x) + v\right) \tag{26}$$

where v is then designed to stabilize $\dot{x} = v$. Such feedback linearization has for example been used in [80, 84] to cancel out aerodynamic forces. However, the linearization based on $f(x)$ and $g(x)$ is highly model dependent and thus rather sensitive to modeling errors and parametric uncertainties, which can affect the stability of the system dramatically [187]. Using an online model estimator, these effects can be mitigated. Depending on the application, different parts of the model are considered as adaptive parameters. Possible implementations include aerodynamic parameter estimation only [53, 54], lumping all nonlinear effects into an equivalent disturbance or robust compensator [91, 92, 95, 94, 93] and full model estimation [59]. A summary of common adaptive parameters and estimation laws is provided in Table 8. Another method to estimate and compensate for model uncertainties in the dynamic inversion approach is to apply machine learning techniques, such as presented for the ducted fan UAV in [45]. The nonlinear model functions $f(x)$ and $g(x)$ from (25) are separated into a known and unknown part, whereby the latter is learned by a NN. Using a Lyapunov stability analysis, boundedness of the tracking error during learning is shown.

A direct extension of observer-based dynamic inversion is presented by *Model Reference Adaptive Control (MRAC)*. As shown in Fig. 17, this scheme uses a reference model with desired tracking performance and adapts the controller according to the difference between the real and reference model [230]. A standard MRAC implementation is presented in [51] to handle nonlinearities in the pitch angle dynamics. Although online estimation allows the controller to adapt to system changes, high estimation gains might negatively affect stability and robustness. This issue is addressed by a new concept called L_1-adaptive control [231, 232, 233], which adds a low-pass filter at a specific point in the control architecture, thereby decoupling the estimation and control loop. This concept has been successfully applied to a tailsitter UAV in [58].

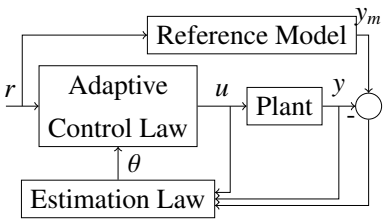

Figure 17: Model-reference adaptive control

The presented adaptive methodologies can be combined with any sort of baseline control law. Tuning examples for P/PD/PID are presented in [84, 53] and for LQR in [83, 82], respectively. The work in [87] explains in detail the combination of observer-based dynamic inversion with backstepping.

A completely model-free control approach is presented in [90], using *Reinforcement Learning* to train a pure NN controller. In this methodology, an agent (hybrid VTOL UAV) takes an action based on its state relative to the environment and a corresponding reward is calculated. The sequence of optimal actions maximizing the cumulative reward is called the optimal policy which is to be learned. In the presented work, the reward function is a combination of velocity tracking error, energy efficiency, flight stability, error integral and vehicle orientation. Training is conducted exclusively in simulation, and no manual tuning of the flight controller was needed between the training simulations and the real-flight tests. The final policy not only achieved successful

transition between hover and cruise flight modes but could also be applied to different platforms as shown in Fig. 18.

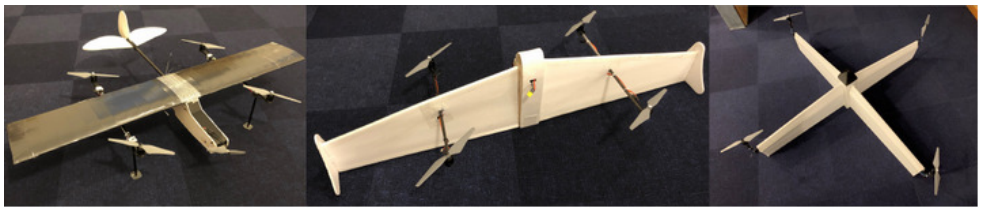

Figure 18: Reinforcement learning has been recently used to train neural networks to control a wide variety of hybrid VTOL aircraft as shown in [90].

5.2.2. Tiltrotor

An initial approach for tiltrotor UAV control was using conservatively tuned Robust Control. As a reference, [99] demonstrates a particle swarm optimization approach to tune the controller gains. Since this algorithm allows to include constraints in the gain and phase margin, rising time and maximum overshoot, stability over the entire flight envelope can be ensured. Stability and robustness over the whole flight envelope could also be proven in [219, 141], using an H_∞ control approach together with a *Linear Parameter Varying* [234] system representation. The corrsponding gain matrix is obtained through μ-synthesis [219] or Lyapunov methods [141]. Further H_∞-like controller designs are found in [111, 218].
Tracking performance can be improved through Direct Gain Scheduling implementations, as shown in [113]. Here, a single neuron NN continuously adapts the gains of a PID controller as shown in Fig. 19. Based on equation (19), the adaptation law takes the form

$$K_j(t) \leftarrow K_j(t) + \eta e(t)^2 \frac{\partial u_{PID}(x(t))}{\partial x(t)} \qquad j \in \{P, I, D\},$$

where η is the learning rate. NN-based Direct Gain Scheduling is also used in [150], where the SMC gains are scaled with the output of a radial-basis function NN to counteract the chattering phenomenon.
As for tailsitters, the addition of nonlinear Dynamic Inversion terms helps to improve flight performance and simplify controller tuning. While some implementations are purely model based [133, 121, 235], newer publications tend more towards the use of data-driven methods. A classical example is the use of extended state observers as shown in [110, 107]. On the other hand, [125] develops an adaptive control strategy, shown in Fig. 20, whereby all model-uncertainty and nonlinearities are lumped into a single compensation term computed by a radial-basis function NN. The results show that modeling errors, CoG-location errors, and

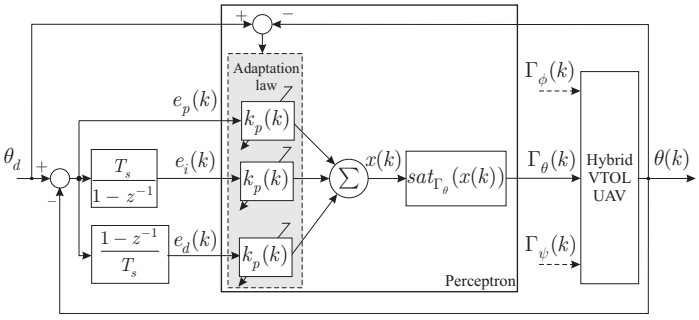

Figure 19: The pitch angle control architecture used in [113]. The pitch torque $\Gamma_\theta(k)$ applied to the aircraft is computed from the pitch angle error $e_\theta(k) = \theta_d(k) - \theta(k)$ and passed through a PID controller whose gains are adapted on line, as being the weights of one-neuron neural network.

inertia-term errors are well compensated. Similar NN-based Dynamic Inversion approaches are presented in [102, 236, 135, 124, 112]. Another machine learning technique known as *iterative learning* is used in [89]. These different formulations for adaptive parameters and corresponding estimation laws in observer-based Dynamic Inversion are collected in Table 8.

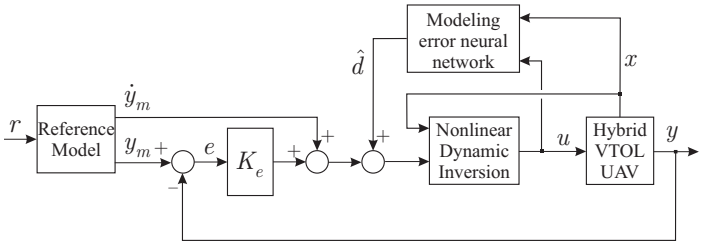

Figure 20: Neural network augmentation for nonlinear *Dynamic Inversion* in [125]

As a promising alternative to the prevailing Dynamic Inversion strategy, recent works have started to look at *Nonlinear Model Predictive Control (NMPC)* for full envelope tiltrotor UAV control [143, 146, 147]. NMPC is an optimal control scheme, implemented in a receding horizon fashion, meaning that an optimization problem of the form:

$$\min_{\substack{\{x_2,\dots,x_{N+1}\}\\ \{u_1,\dots,u_N\}}} \sum_{j=1}^{N} h_j(x_j,u_j) + h_{N+1}(x_{N+1}) \tag{27a}$$

$$s.t. \quad \dot{x} = f(x,u) \tag{27b}$$

$$x_1 = x(t) \tag{27c}$$

$$x_j \in \mathcal{X}\ \forall j \in \{1,\dots,N+1\} \tag{27d}$$

$$u_j \in \mathcal{U}\ \forall j \in \{1,\dots,N\} \tag{27e}$$

with finite prediction horizon N is reinitialized (27c) and solved at every iteration [237]. As shown in [143, 146, 147], the problem formulation allows the inclusion of the full nonlinear system model (including aerodynamic and coupling effects, as well as potential tilt angle dynamics) together with vehicle specific state (27d) and actuator (27e) constraints.

5.2.3. Tiltwing

Unfortunately, literature on unified control laws for tiltwing vehicles is still rather sparse. The few academic works which successfully cover the full flight envelope with a single controller, follow the same patterns as introduced above. For example, [166] very well shows the controller synthesis process for a model-based Dynamic Inversion approach with a baseline LQR controller. Adaptive parameter formulations and corresponding estimation laws for observer-based *Dynamic Inversion* are presented in Table 8.
Similar to tiltrotor vehicles, a recent work investigates the use of NMPC for autonomous tiltwing control [155]. Herein, the full development process covering system modeling, parameter estimation and identification, trim-map generation for NMPC regularization and finally the NMPC design and implementation itself is discussed in detail.

5.3. Flight Performance Comparison between a Scheduled vs. a Unified Control Approach

The scheduled and unified control approaches presented in Sections 5.1 and 5.2 respectively compose two fundamentally different methodologies for hybrid UAV control. To provide some intuition about the flight

Table 5: Tailsitter control methods

Control Methodology	Description	Source
Separate Control Approach	Divide and Conquer with P/PD/PID	[32, 41, 65, 71, 72, 77, 78, 213, 226, 238, 239]
	Divide and Conquer with LQR	[32, 55, 64, 67, 68]
	Divide and Conquer with Backstepping	[61]
	Control Authority Weighting with P/PD/PID	[49]
Unified Control Approach	Robust Control	[34, 52, 56, 66, 70, 76]
	Direct Gain Scheduling with P/PD/PID	[36]
	Dynamic Inversion with P/PD/PID	[94, 95, 81, 59, 48, 84, 60, 74, 44, 37, 88, 53, 54, 62, 73, 75, 80, 45, 89]
	Dynamic Inversion with LQR	[93, 91, 92, 82, 83]
	Dynamic Inversion with Backstepping	[31, 33, 38, 87, 216]
	Model Reference Adaptive Control	[58, 51, 30]
	Reinforcement Learning	[90]

Table 6: Tiltrotor control methods

Control Methodology	Description	Source
Separate Control Approach	Divide and Conquer with P/PD/PID	[117, 132, 138, 149, 240]
	Divide and Conquer with LQR	[100, 101, 105, 106, 220, 222, 227, 241]
	Divide and Conquer with SMC	[109, 228]
	Control Authority Weighting with P/PD/PID	[130, 131, 142, 144]
	Control Authority Weighting with LQR	[140]
Unified Control Approach	Robust Control	[120, 218, 242, 122, 243, 223, 99, 111]
	Linear Parameter Varying with H_∞	[141, 219]
	Direct Gain Scheduling with SMC	[150]
	Direct Gain Scheduling with P/PD/PID	[113]
	Dynamic Inversion with P/PD/PID	[133, 102, 135, 236, 235, 244, 104, 96, 97, 125, 112]
	Dynamic Inversion with SMC	[110, 121]
	Dynamic Inversion with Backstepping	[136, 137]
	Nonlinear Model Predictive Control	[147, 146]

Table 7: Tiltwing control methods

Control Methodology	Description	Source
Separate Control Approach	Divide and Conquer with P/PD/PID	[151, 153, 154, 165]
	Divide and Conquer with H_∞	[171, 172, 173, 174, 175]
	Control Authority Weighting with P/PD/PID	[156]
Unified Control Approach	Dynamic Inversion with P/PD/PID	[160, 161]
	Dynamic Inversion with LQR	[166]
	Model Reference Adaptive Control	[167]
	Nonlinear Model Predictive Control	[155]

performance and difference thereof, this section will compare and discuss the simulation results of a representative state-of-the-art controller from each section. As a comparison platform, a high-fidelity simulator of

Table 8: Collection of common adaptive parameters and estimation laws in the observer-based *Dynamic Inversion* unified control approach for hybrid UAV control

Type	Adaptive Parameters	Estimation Law	Source
Tailsitter	Affine Model Parameters	Inverse Laplace Transform	[59]
	Aerodynamic Effects	Filtered Plant Inversion	[74]
	Equivalent Disturbance	Filtered Plant Inversion	[91, 92, 83, 82, 95, 94, 93]
	Aerodynamic Effects	Extended State Observer	[87]
	Equivalent Disturbance	Luenberger/Kalman Observer	[37]
	Aerodynamic Coefficients	Luenberger/Kalman Observer	[53, 54]
	Affine Model Parameters	Recursive Least Squares	[31, 33]
	Affine Model Parameters	Lyapunov-based Design	[44, 216, 58]
	Equivalent Disturbance	Lyapunov-based Design	[30, 51]
Tiltrotor	Equivalent Disturbance	Neural Networks	[236, 102, 135, 89, 112, 124]
	Equivalent Disturbance	Extended State Observer	[96, 97, 104, 110]
Tiltwing	Equivalent Disturbance	Filtered Plant Inversion	[161, 160]
	Affine Model Parameters	Lyapunov-based Design	[167]

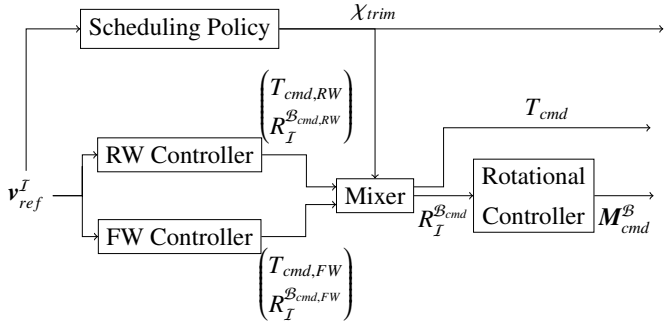

(a) FPID scheduled control approach: Given a desired reference velocity $v_{ref}^{\mathcal{I}}$, two independent RW and FW controllers compute total thrust commands $T_{cmd,RW}, T_{cmd,FW}$ and reference attitudes $R_{\mathcal{I}}^{\mathcal{B}_{cmd,RW}}, R_{\mathcal{I}}^{\mathcal{B}_{cmd,FW}}$ for thrust vector alignment each. As usual for scheduled control approaches, the rotor-tilt angle is considered constant in each controller and not used for improved thrust vector alignment. Instead, the scheduling policy continuously adapts the rotor-tilt angle χ_{trim} as a linear function of the desired velocity and then nonlinearly mixes the RW and FW contributions.

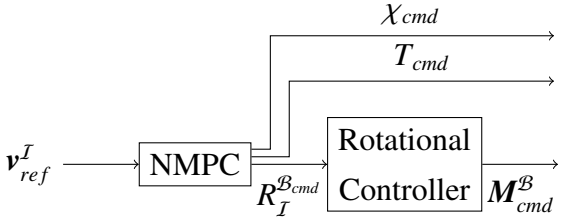

(b) NMPC unified control approach: Given a desired reference velocity $v_{ref}^{\mathcal{I}}$, the underlying optimization problem continuously solves for the combination of total thrust T_{cmd}, rotor-tilt angle χ_{cmd} and attitude $R_{\mathcal{I}}^{\mathcal{B}_{cmd}}$ commands which yields the desired trade-off between tracking performance and efficiency. A simplified version of the vehicle dynamics is used inside the NMPC formulation to allow real-time online deployment. Since the tilt angle and attitude are computed online at the same time, the overall flight performance can be improved compared to purely static tilt angle maps.

Figure 21: Representative state-of-the-art scheduled and unified control approaches

the tiltrotor vehicle shown in Fig. 6 has been developed, based on the detailed vehicle model derived in [134]. Amongst other things, the simulation includes precise aerodynamic models of the wing, fuselage, stabilizers and control surfaces, gyroscopic effects and inherent dynamics of the tilting actuation, as well as changes in propeller thrust generation due to airspeed.

As an exemplary scheduled control approach, the recently developed FPID implementation is selected [144]. As sketched and explained in Fig. 21a, the method uses the Control Authority Weighting scheduling policy. Similarly, the latest development in unified control approaches is given by the novel NMPC algorithm described in [143, 146] and portrait in Fig. 21b. Although both control approaches have been successfully tested in outdoor experiments, the simulator mentioned above is used here to ensure a fair comparison. Furthermore, both methods use the same control allocation strategy and are commanded to track the exact same trajectory, namely a constant acceleration for RW-to-FW and constant deceleration for FW-to-RW transitions. Each controller has been tuned to achieve best performance respectively. The simulation results of the two approaches are shown in Fig. 22.

Due to the inherent linearization and statically-determined rotor-tilt angle commands of scheduled control

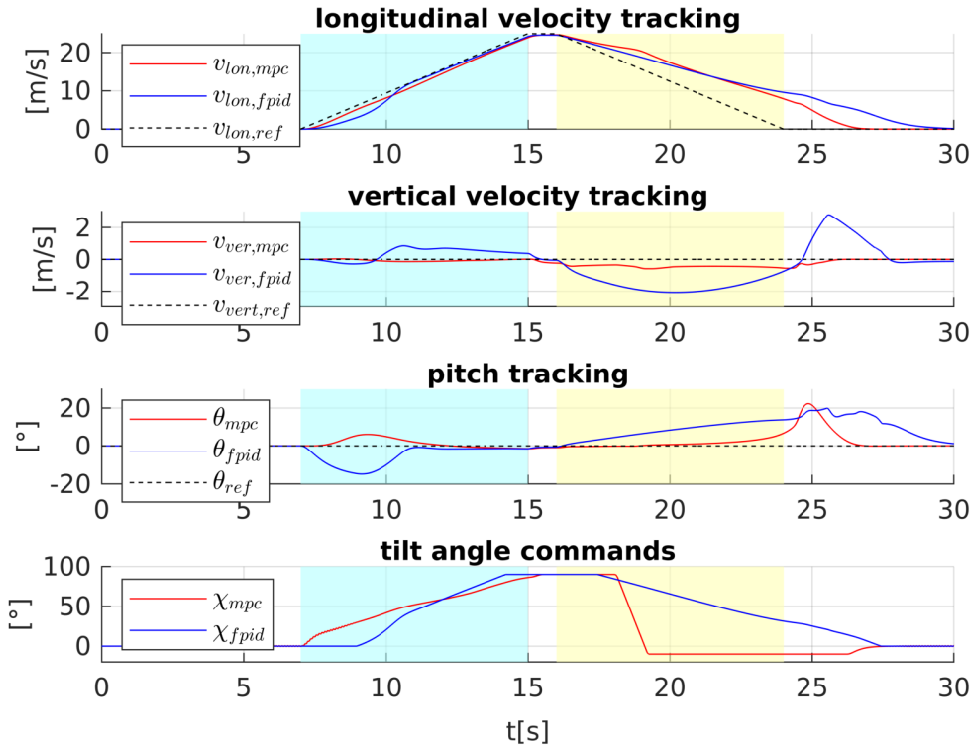

Figure 22: Simulation results comparing NMPC and FPID performance during transition phases with acceleration and deceleration phase highlighted in cyan and yellow, respectively

approaches, the FPID controller initially accelerates the vehicle by pitching down, as if it were a regular multicopter ($t = 7\text{s} - 11\text{s}$). However, this maneuver results in undesired downwards lift forces being generated by the main wing (see Section 4.2). On the other hand, the combined tilt angle and attitude computation in the NMPC controller accelerates the vehicle only through increasing tilt angles. In addition, the fixed airspeed-dependent mapping of the rotor-tilt angle in the FPID control approach has the main drawback that, as long as the airspeed remains high, the rotors are not commanded to tilt back to the RW configuration. This results in a very slow speed decrease and poor vertical tracking compared to NMPC ($t = 24\text{s} - 27\text{s}$).

In summary, the unified NMPC control approach outperforms the scheduled FPID methodology in all flight phases. On the one hand, this is related to the fundamental difference in tilt angle computation between scheduled and unified controllers. While the former use static mappings (hand-crafted or trim-point based), the latter allow an online adaptive and thus potentially more optimal design. On the other hand, the discretization of the flight envelope in scheduled control approaches means that the knowledge of the model is incomplete. Thus, control performance is affected, especially in between the selected operating points. In unified control approaches and NMPC in particular, the full model is included to optimize the control sequence. For a more detailed discussion, the interested reader is referred to [146].

This analysis confirms the observable trend in academia, moving towards nonlinear, unified approaches. However, the superiority of such methods strongly relies on the accuracy of the underlying model. In case a high-quality system identification is not possible, machine learning or general data-driven methods are used to mitigate these effects as mentioned in Section 5.2.

More advanced and optimization-based approaches might also come at the cost of increased computational load. In practice, this might require a powerful on-board companion computer, while the simple scheduled control implementations can run directly on standard-available autopilots.

Table 9: Actuation effects on translational and rotational motion

Hybrid UAV	Actuator Command	VTOL Mode		Cruise Mode	
		transl. motion	rot. motion	transl. motion	rot. motion
Tailsitter	Synchronous Rotor Thrust	vertical	-	horizontal	-
	Differential Rotor Thrust	lateral	yaw	lateral	yaw
	Synchronous Elevon Deflection	horizontal	pitch	vertical	pitch
	Differential Elevon Deflection	-	roll	lateral	roll
Tiltrotor	Synchronous Rotor Thrust	vertical	-	horizontal	-
	Differential Rotor Thrust	lateral	roll	lateral	yaw
	Synchronous Elevon Deflection	-	-	vertical	pitch
	Differential Elevon Deflection	-	-	lateral	roll
	Synchronous Tilting	horizontal	-	vertical	-
	Differential Tilting	-	yaw	lateral	roll
Tiltwing	Synchronous Rotor Thrust	vertical	-	horizontal	-
	Differential Rotor Thrust	lateral	roll	lateral	yaw
	Synchronous Elevon Deflection	horizontal	pitch	vertical	pitch
	Differential Elevon Deflection	-	yaw	lateral	roll
	Synchronous Tilting	horizontal	-	vertical	-
	Differential Tilting	-	yaw	lateral	roll

6. Control Allocation

The goal of control allocation is to map the virtual commands generated by the flight controller to all the available actuators of the flying vehicle. The redundancies between rotors, tilt angles and aerodynamic control surfaces need to be adequately employed, especially when the control authority depends on the flight conditions. As an example, the aerodynamic control surfaces have more control authority as the airflow speed passing over them increases. A detailed list of how the different actuators affect the translational and rotational dynamics in each flight mode can be found [245, 134] and in the summary provided in Table 9 .

6.1. Control Allocation for Tailsitter Aircraft

The control allocation process in tailsitter vehicles depends on whether aerodynamic control surfaces are used for maneuvering or not. Table 3 summarizes the designs encountered in literature. Both approaches are considered below.

6.1.1. Control Allocation for Tailsitter with Rotors, no Elevon

Similar to conventional multicopters, the individual rotor speeds can be statically mapped to virtual body forces and moments, as has been done in [76, 77, 91, 80, 95, 82, 83, 92, 94, 93]. If the rotors are mounted symmetrically such as for the prototype in Fig. 23, this relation can be written as:

$$\underbrace{\begin{pmatrix} u_F \\ u_{M1} \\ u_{M2} \\ u_{M3} \end{pmatrix}}_{\boldsymbol{u}} = \underbrace{\begin{pmatrix} c_F & c_F & c_F & c_F \\ c_M & -c_M & c_M & -c_M \\ lc_F & lc_F & -lc_F & -lc_F \\ -lc_F & lc_F & lc_F & -lc_F \end{pmatrix}}_{M} \underbrace{\begin{pmatrix} \omega_1^2 \\ \omega_2^2 \\ \omega_3^2 \\ \omega_4^2 \end{pmatrix}}_{\boldsymbol{\omega}} \tag{28}$$

with thrust and drag coefficients c_F, c_M and moment arm l. Further, the individual rotor speeds are denoted as ω_i and $\boldsymbol{u}$ are the virtual control inputs. Hereby, u_F denotes the total thrust parallel to the main body axis, while u_{Mi} are roll, pitch and yaw moment respectively. Since the matrix M in (28) has full rank, the actuator

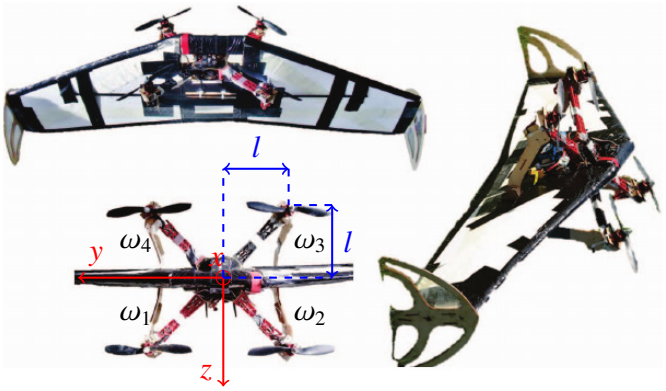

Figure 23: Tailsitter with four rotors, no elevon [78]

commands $\boldsymbol{\omega}_c$ can be easily computed from the controller output $\boldsymbol{u}_c$ as:

$$\boldsymbol{\omega}_c = M^{-1}\boldsymbol{u}_c \tag{29}$$

which was used in [88, 73].

6.1.2. *Control Allocation for Tailsitter with Rotors and Elevons*

The works in [226, 213, 57, 59, 55] present a matrix-inversion based allocation method. However, the matrix is no longer static, since the lift and drag coefficients of the elevons are state-dependent. As an example, the following set of equations is used in [57] for the prototype shown in Fig. 24:

$$\underbrace{\begin{pmatrix} u_F \\ u_{M1} \\ u_{M2} \\ u_{M3} \end{pmatrix}}_{\boldsymbol{u}} = \underbrace{\begin{pmatrix} c_{F,\omega} & c_{F,\omega} & 0 & 0 \\ 0 & 0 & -c_{M1,\delta}(\boldsymbol{x}) & c_{M1,\delta}(\boldsymbol{x}) \\ 0 & 0 & c_{M2,\delta}(\boldsymbol{x}) & c_{M2,\delta}(\boldsymbol{x}) \\ lc_{F,\omega} & -lc_{F,\omega} & 0 & 0 \end{pmatrix}}_{M(\boldsymbol{x})} \begin{pmatrix} \omega_1^2 \\ \omega_2^2 \\ \delta_1 \\ \delta_2 \end{pmatrix} \tag{30}$$

with surface deflections δ_1 and δ_2 and where the elevon coefficients $c_{M1,\delta}$ and $c_{M2,\delta}$ are modeled as state $\boldsymbol{x}$ dependent parameters. As a consequence, the matrix inverse needs to be recomputed at each iteration.
A slightly modified approach is shown in [72] for the example of a tailsitter with four propellers and two elevons. In that work, a velocity-dependent scale is used to distribute the required moments between the rotors and the elevons. This way, one can account for the changing control authority and ensure efficient flight.

An interesting concept is presented in [246], which consists in a morphing tailsitter design, as shown in Fig. 25. The vehicle can take the shape of a large wing for solar-powered cruise flight in FW mode. During VTOL operation on the other hand, the vehicle can reconfigure itself into a compact multi-rotor-like airframe. A nonlinear mixer module is used to distribute the control actions between rotor speeds, control surface deflections and the hinge-actuation servos.

6.1.3. *Automatic Control Allocation for Tailsitter Aircraft*

In case a vehicle has an entire set of primary control-surfaces available, rather than just a pair of elevons, the attitude dynamics can be decoupled by directly mapping the required moments to the corresponding control-surfaces. In other words, roll commands are passed to ailerons, pitch commands to elevators and

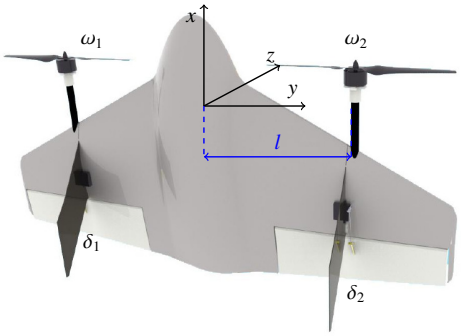

Figure 24: Tailsitter simultaneous rotor and elevon allocation example [57]

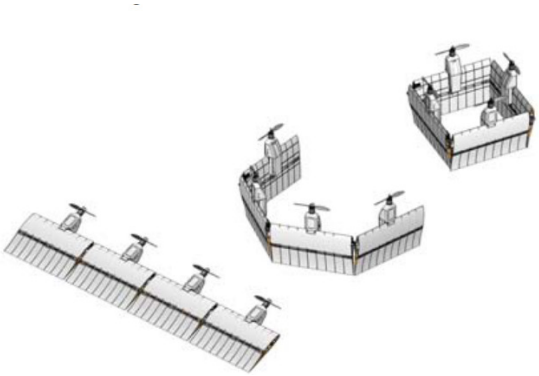

Figure 25: Morphing tailsitter design [246]

yaw commands to the rudder. This combination of controller and allocation has been used in ducted-fan or wing-fuselage designs by [31, 32, 30, 33, 46, 34, 35, 40, 44, 68, 41, 36, 42, 37, 52, 38].

6.2. Control Allocation for Tiltrotor Aircraft

Numerous works have shown how effects of the rotor-tilt angles, rotor speeds and control-surface actuators can be lumped into virtual body forces and moments [131, 132, 127, 113, 133, 136, 134, 138, 106, 139, 140, 119, 240, 149, 143, 146]. In turn, control allocation consists in mapping the desired virtual forces and moments generated by the flight controllers to actual actuator control signals. In the case of tiltrotor aircraft, the actuation is provided by rotor speeds, control surfaces and rotor tilting.

Control allocation for tiltrotor VTOL UAVs can be divided into the two main approaches found in the literature. In the first approach, if there are enough DoF, the rotor-tilt angles can be ignored in the allocation procedure, meaning that only rotor thrust and control-surface deflections are used for stabilization. The second approach exploits explicitly the rotor-tilt angle as part of the control allocation algorithm. Both approaches are detailed below.

6.2.1. Approach 1: Allocation Excluding Rotor-tilt Angle

This approach can only be pursued if the rotors provide sufficient thrust to control the vehicle in the VTOL mode. This is the case for a four-rotor vehicle as shown in Fig. 6 or a tri-copter with laterally tiltable-tail propeller as shown in Fig. 26. For these UAVs, the approach reported in [130, 135, 118] provides an equation similar to (28), allowing actuator command computation through matrix inversion.

The work in [117] allocates rotor speeds and elevon deflections using a model-inversion approach to track the virtual roll-, pitch- and yaw-desired moments. A similar approach is found in [107], where model inversion is used to compute actuator commands for all primary control-surfaces. The algorithm employed in [142] distributes the torque control actions between differential rotor thrust and control-surface deflection, based on

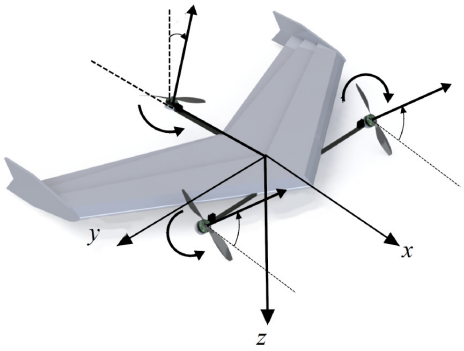

Figure 26: Tri-copter with laterally tiltable tail propeller [118]

an airspeed-dependent gain. The works in [143, 145, 147, 146] use a daisy-chaining approach, where energy-cheap actuators, namely aerodynamic control surfaces, are prioritized over propeller thrusts. In addition, differential rotor-tilt angle is used to generate a motion around the thrust axis, resulting in an efficient way to produce high-yaw torque without resorting to propeller differential thrusts. To reduce complexity, [242, 247] simply weight the control-surface commands with airspeed-dependent gains to account for the changing control authority.

6.2.2. Approach 2: Allocation Including Rotor-tilt Angle

If the vehicle can not be stabilized in VTOL mode by exclusively changing the rotor speeds, the tilt angles need to be included in the allocation.

Three-rotor Tilting UAVs with rigidly-mounted tail rotor as shown in Fig. 27 often use the tilt angles to yaw, without inducing a roll moment. This approach is used in [115, 116, 121]. Additionally, [126, 129, 128] achieve longitudinal force generation by tilting the rotors, rather than pitching the vehicle.

Two-rotor Tilting Aircraft suffer from the same lack of controllability and also require propeller tilt angle allocation, for example via pseudo-inverse matrix as shown in [111].

In cruise mode, the rotor-tilt angles can be neglected in the allocation, since the combination of rotor speed and control-surface deflection provides enough control authority to track the stabilizing commands.
During transition maneuvers however, tilt angle, rotor speed and surface deflection are often all mixed together, with the individual contributions weighted according to the current flight conditions [99, 104, 105]. The approach in [109] uses a tilt-angle-dependent gain to distribute a virtual elevator command between tilt angles and control-surfaces. In [120, 96, 97], the allocation among actuators is weighted as a function of airspeed. Additionally, a decoupling mechanism, based on the relationship between tilt angles and differential motor thrust, ensures independence between roll and yaw motions.

Finally, the approach of [141] solves an optimization problem to achieve the most efficient allocation possible.

6.2.3. Direct Control Allocation for Tiltrotor UAVs

Besides the mentioned mappings between virtual controller outputs and actual actuator commands, there exist structures which directly combine controller and allocation. These approaches are often encountered when a linearized system model is used for the controller, such as with Divide and Conquer (see Section 5.1.1)

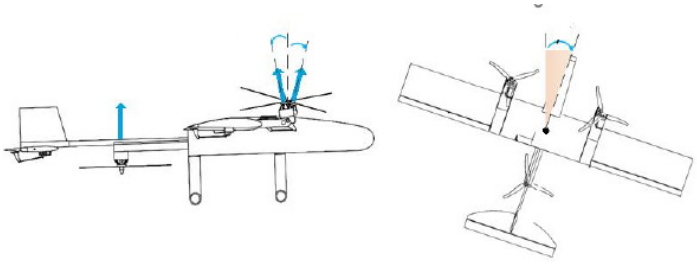

Figure 27: Yaw motion for three-rotor UAV with rigidly mounted tail rotor[116]

for example. As shown in [227, 218, 228, 241, 217, 219, 114, 220, 171], the control signals for the tilt angle, the rotors' speed and the control-surface angles are directly provided by the controller, and no further manipulation is required.

6.3. Control Allocation for Tiltwing Aircraft

Similarly to tiltrotor vehicles, tiltwing-UAV actuator commands are a combination of feedback stabilization and feedforward action. Additionally, it is also common to use virtual forces and moments in the controller, which has been demonstrated by [157, 162, 164, 168, 152, 169, 170, 248]. The main difference is that the control surfaces for tiltwing vehicles are always in the propeller slipstream, meaning that they have control authority in VTOL mode. As a consequence, the tilt angles are exclusively used in feedforward action. Thus, feedback stabilization can be achieved in all flight conditions using rotor-speed commands only and control-surface deflection.

6.3.1. Tilt Angle Excluding Allocation

The prototype used in [165, 167] has no need for aerodynamic-control surfaces, since full controllability is provided by the four strategically-placed rotor-wing assemblies (similar to the prototype shown in Fig. 4b) . A state-dependent matrix inversion is used to determine the individual rotor speeds from given desired body forces and torques.

The approach presented in [158, 163] distributes the control action between the rotors and aerodynamic-control surfaces depending on the tilt angle, in order to improve the efficiency of the allocation. Along the same lines, [166] uses a model-inversion-based method to obtain rotor speed and flaps commands. Finally, [154] employs so-called *daisy chaining* control allocation method. The actuators are sequentially allocated based on a predefined order of priority, whereby higher priority is assigned to the aerodynamic-control surfaces, for energy efficiency.

6.3.2. Automatic or Direct Allocation for Tiltwing UAVs

Similar to the case with tiltrotor vehicles, automatic allocation is commonly used when a linearized model is derived for the controller synthesis. The respective controller outputs can directly be fed to the actuators, such as demonstrated in [172, 173, 174, 175, 159, 153, 171, 249].

7. Conclusion

This paper reviewed the major currently-available designs for hybrid or convertible VTOL UAVs, together with state-of-the-art flight control methodologies encountered in recent literature. The comparative study has been conducted on the three main different types of hybrid VTOL aircraft, namely 1) tailsitters, 2) tilting-rotors, and 3) tiltwing vehicles. Each class displays inherent advantages and drawbacks over the others,

regarding mechnical complexity, stability, efficiency and maneuverability.
This study shows that the simplest design is the tailsitter type with either two propellers and two elevons, or four propellers and no elevons. As their name indicates, tailsitters require the fuselage to change orientation during flight mode transition. Although they allow efficient wing design, tailsitters also display high susceptibility to wind disturbances during the take off, hover, and landing phases, because of a large vertical wing surface exposed to side winds. On the other hand, the tiltrotor and tiltwing configurations require complex tilting actuation to achieve transition between flight modes. While tiltrotor hybrid UAV are generally less efficient than the other two types, studies also show that it is the most agile and less-wind-susceptible vehicle during the (quasi-)stationary flight phases. In particular, designs with a pair of propellers on each side of the fuselage offer the possibility to produce extra yaw torque by differential-tilting propeller pairs on each side of the fuselage.

This review also focused on the four main components that make up a successful flight control system for an autonomous VTOL aircraft. They are namely: a rigorously-designed 1) physical model of the flying system, 2) reference-trajectory generation during flight mode transition, 3) flight controller and 4) actuator-control allocation.
A highly-nonlinear model is required to accurately capture the combined lift generation from the propellers and wings in the different flight phases. During the transitions from RW mode to FW mode and back, hybrid UAVs encounter large AoA and slow-translational speed flight conditions, during which there are large aerodynamic-lift force variations. These complex dynamics make the generation of reference signals for hybrid VTOL aircraft more challenging compared to conventional RW or FW vehicles alone. In addition, the following constraints must be taken into account: a) physical vehicles limitations such as the limited power or thrust provided by the motors, b) the under-actuated nature of the flying machines, and c) the (strong) nonlinearities and uncertainties in the equations that describe the behavior of the flying machines for the full flight envelope.
In order to handle the varying flight conditions, this study revealed there are two main families of flight control approaches, namely 1) *controller-scheduling* policies, and 2) *unified-control* policies. In the first family of control architectures, separate flight controllers are activated successively or blended depending on the flight operating conditions. These controllers are based on a linearized system model at different operating points or *trim points* within the flight envelope. Those trim points are then scheduled together with the corresponding linear controllers throughout the flight modes. Recent investigations to augment or replace these controllers with data-driven methods and machine learning promise to increase the robustness with respect to modeling and system identification errors.
The second main family of control architecture involves *unified-control* policies without the need to switch among flight controllers. It consists in a continuous single control approach a) valid in all flight modes (VTOL, cruising) despite the fundamental behavior differences between them, b) able to transition between these modes in a controlled, smooth and safe manner, c) robust against model uncertainties and unpredictable external perturbations. To this end, the current trend is to incorporate as much knowledge of the vehicle as possible into the flight controller, for example through highly-nonlinear control laws, model predictive control, neural networks or machine learning approaches. These methods remove the need to schedule offline-precomputed controllers, but rather they are able to capture and exploit the nonlinearities of the system and compute control signals that can take into account the vehicle's physical limitations simultaneously, in realtime.

To conclude, control system design for hybrid UAVs is still a very active field in modern research. Only

a few projects have successfully completed their development phase and are ready to be used in real-world applications. Current and future development concentrate on elaborated more sophisticated approaches, both to improve model fidelity and control performance. This is done through combination of data-driven, model-based, optimization and self-learning flight control approaches. However, such approaches often require more computing power aboard the vehicle. Although processors keeps increasing in speed and memory, it is still required to mitigate control complexity and available computing resources.

Interests Statement

The authors declare that they have no known competing financial interests or personal relationships that could have appeared to influence the work reported in this paper.

References

[1] A. Reinhard, Door to Door 4D Mobilität vom Fliegenden Auto zum Air-taxi, AS Verlag, ISBN: 978-3-906055-99-2, 2019.

[2] Military History Matters, Back to the drawing board: The Lockheed XFV-1 Salmon, accessed 2021 (2012).
URL https://www.military-history.org/articles/back-to-the-drawing-board-the-lockheed-xfv-1-salmon.htm

[3] Wikipedia contributors, Lockheed XFV, accessed 2021 (2019).
URL https://en.wikipedia.org/wiki/Lockheed_XFV

[4] M. Taylor, Jane's Encyclopedia of Aviation, London: Studio Editions, 1989.

[5] Wikipedia contributors, Vertol VZ-2, accessed 2021 (2021).
URL https://en.wikipedia.org/wiki/Vertol_VZ-2

[6] RAF Historical Society, The RAF Harrier Story, Advanced Book Printing, 2006.

[7] Wikipedia contributors, Harrier Jump Jet, accessed (2021).
URL https://en.wikipedia.org/wiki/Harrier_Jump_Jet

[8] Dassault, Dassault Aviation, Mirage III V, origins and prototypes, accessed 2021.
URL https://www.dassault-aviation.com/fr/passion/avions/dassault-militaires/mirage-iii-v/

[9] Wikipedia contributors, Dassault Mirage IIIV (2021).
URL https://en.wikipedia.org/wiki/Dassault_Mirage_IIIV

[10] S. Markman, B. Holder, Bell/Boeing V-22 Osprey Tilt-Engine VTOL Transport (U.S.A.). Straight Up: A History of Vertical Flight., Schiffer Publishing, Atglen 2000, ISBN 0-7643-1204-9, 2000.

[11] Wikipedia contributors, Bell-Boeing V-22 (2021).
URL https://de.wikipedia.org/wiki/Bell-Boeing_V-22

[12] J. Hamstra, The F-35 Lightning II: From Concept to Cockpit., American Institute of Aeronautics and Astronautics (AIAA), 2019.

[13] Wikipedia contributors, Lockheed Martin F-35 Lightning II (2021).
URL https://en.wikipedia.org/wiki/Lockheed_Martin_F-35_Lightning_II

[14] Aviation Week Network, Sikorsky's Rotor Blown Wing – Look Familiar? (2013).
URL https://aviationweek.com/sikorskys-rotor-blown-wing-look-familiar

[15] Darren Quick, Israel Aerospace Industries unveils tilt-rotor Panther UAV platform (2010).
URL https://newatlas.com/tilt-rotor-panther-uav/16619/

[16] Matthew Monaghan, Aurora wins DARPA VTOL X-Plane program contract (2014).
URL https://www.sae.org/news/2014/02/aurora-wins-darpa-vtol-x-plane-program-contract

[17] Boeing, Boeing Phantom Swift Selected for DARPA X-Plane Competition (2014).
URL https://boeing.mediaroom.com/Boeing-Phantom-Swift-Selected-for-DARPA-X-Plane-Competition

[18] Vertiflite, Project Zero: The exclusive story of AgustaWestland's 'all-electric technology incubator. 59 (3) (June 2013).
URL https://en.wikipedia.org/wiki/AgustaWestland_Project_Zero

[19] Aurora Flight Sciences, LightningStrike XV-24A Demonstrator Successfully Completes Subscale Flight Test Program (April 4 2017).

[20] Wingcopter, Wingcopter Specsheet (2010).
URL https://wingcopter.com/wp-content/uploads/2020/03/Specsheet_Wingcopter_178HL-2.pdf

[21] Wingtra, WingtraOne - mapping drone for high-accuracy aerial surveys, accessed 2021 (2020).
URL https://wingtra.com/mapping-drone-wingtraone/#intro

[22] Airbus, Airbus Commercial Aviation : Vahana, Our Single-seat eVTOL Demonstrator, accessed 2021.
URL https://www.airbus.com/innovation/zero-emission/urban-air-mobility/vahana.html

[23] P. Poisson-Quiton, Introduction to V/STOL Aircraft Concepts and Categories, AGARDograph 126 (May 1968).

[24] S. Anderson, Historical Overview of V/STOL Aircraft Technology, NASA Ames Research Center: NASA Technical Memorandum (March 1981).

[25] M.J. Hirshcherg, V/STOL: The First Half-Century, Vertiflite, accessed 2021 (March/April 1997).
URL https://studylib.net/doc/8542802/v-stol--the-first-half-century-by-michael-j.-hirschberg-f...

[26] Y. Zhou, H. Zhao, Y. Liu, An evaluative review of the vtol technologies for unmanned and manned aerial vehicles, Computer Communications 149 (2020) 356–369. doi:https://doi.org/10.1016/j.comcom.2019.10.016.
URL https://www.sciencedirect.com/science/article/pii/S014036641930996X

[27] Advisory Group for Aerospace Research & Development (AGARD), Agard report no. 577 on v/stol handling, i- criteria and discussion (1970).

[28] Wikipedia contributors, Accidents and Incidents Involving the V22 Osprey, accessed January 2021.
URL https://en.wikipedia.org/wiki/Accidents_and_incidents_involving_the_V-22_Osprey

[29] W. E. Green, P. Y. Oh, A MAV that flies like an airplane and hovers like a helicopter, in: Proceedings, 2005 IEEE/ASME International Conference on Advanced Intelligent Mechatronics., 2005, pp. 693–698. doi:10.1109/AIM.2005.1511063.

[30] S. R. Osborne, Transitions between hover and level flight for a tailsitter UAV, Master's thesis, Brigham Young University (2007).

[31] N. B. Knoebel, Adaptive quaternion control of a miniature tailsitter UAV, Master's thesis, Brigham Young University (August 2007).

[32] A. Frank, J. Mcgrew, M. Valenti, D. Levine, J. How, Hover, transition, and level flight control design for a single-propeller indoor airplane, American Institute of Aeronautics and Astronautics (08 2007). doi:10.2514/6.2007-6318.

[33] N. B. Knoebel, T. W. McLain, Adaptive quaternion control of a miniature tailsitter UAV, in: 2008 American Control Conference, 2008, pp. 2340–2345. doi:10.1109/ACC.2008.4586841.

[34] W. E. Green, P. Y. Oh, A hybrid MAV for ingress and egress of urban environments, IEEE Transactions on Robotics 25 (2) (2009) 253–263. doi:10.1109/TRO.2009.2014501.

[35] T. Matsumoto, K. Kita, R. Suzuki, A. Oosedo, K. Go, Y. Hoshino, A. Konno, M. Uchiyama, A hovering control strategy for a tail-sitter VTOL UAV that increases stability against large disturbance, in: 2010 IEEE International Conference on Robotics and Automation, 2010, pp. 54–59. doi:10.1109/ROBOT.2010.5509183.

[36] B. D. Marchini, Adaptive control techniques for transition-to-hover flight of fixed-wing UAVs, Master's thesis, California Polytechnic State University (2013).

[37] S. Kohno, K. Uchiyama, Design of robust controller of fixed-wing UAV for transition flight, in: 2014 International Conference on Unmanned Aircraft Systems (ICUAS), 2014, pp. 1111–1116. doi:10.1109/ICUAS.2014.6842364.

[38] W. Wang, J. Zhu, M. Kuang, Design, modelling and hovering control of a tail-sitter with single thrust-vectored propeller, in: 2017 IEEE/RSJ International Conference on Intelligent Robots and Systems (IROS), 2017, pp. 5971–5976. doi:10.1109/IROS.2017.8206492.

[39] Z. Omar, C. Bil, R. Hill, The application of fuzzy logic on transition manoeuvre control of a new ducted-fan VTOL UAV configuration, in: Second International Conference on Innovative Computing, Informatio and Control (ICICIC 2007), 2007, pp. 434–434. doi:10.1109/ICICIC.2007.562.

[40] A. Manouchehri, H. Hajkarami, M. S. Ahmadi, Hovering control of a ducted fan vtol unmanned aerial vehicle (UAV) based on PID control, in: 2011 International Conference on Electrical and Control Engineering, 2011, pp. 5962–5965. doi:10.1109/ICECENG.2011.6057155.

[41] M. E. Argyle, R. W. Beard, S. Morris, The vertical bat tail-sitter: Dynamic model and control architecture, in: 2013 American Control Conference, 2013, pp. 806–811. doi:10.1109/ACC.2013.6579935.

[42] J. M. Beach, M. E. Argyle, T. W. McLain, R. W. Beard, S. Morris, Tailsitter attitude control using resolved tilt-twist, in: 2014 International Conference on Unmanned Aircraft Systems (ICUAS), 2014, pp. 768–779. doi:10.1109/ICUAS.2014.6842322.

[43] S. Deng, S. Wang, Z. Zhang, Aerodynamic performance assessment of a ducted fan uav for vtol applications, Aerospace Science and Technology 103 (2020) 105895. doi:https://doi.org/10.1016/j.ast.2020.105895.
URL https://www.sciencedirect.com/science/article/pii/S1270963820305770

[44] Y. Jung, D. Shim, Development and application of controller for transition flight of tail-sitter UAV, Journal of Intelligent & Robotic Systems 65 (1-4) (2012) 137–152.

[45] Z. Cheng, H. Pei, S. Li, Neural-networks control for hover to high-speed-level-flight transition of ducted fan uav with provable stability, IEEE Access 8 (2020) 100135–100151. doi:10.1109/ACCESS.2020.2997877.

[46] J. A. Guerrero, R. Lozano, G. Romero, D. Lara-Alabazares, K. C. Wong, Robust control design based on sliding mode control for hover flight of a mini tail-sitter unmanned aerial vehicle, in: 2009 35th Annual Conference of IEEE Industrial Electronics, 2009, pp. 2342–2347. doi:10.1109/IECON.2009.5415267.

[47] J. Escareno, S. Salazar, E. Rondon, Unmanned Aerial Vehicles: Embedded Control, Wiley, 2010, Ch. 3, pp. 41–58.

[48] S. Verling, B. Weibel, M. Boosfeld, K. Alexis, M. Burri, R. Siegwart, Full attitude control of a VTOL tailsitter UAV, in: 2016 IEEE International Conference on Robotics and Automation (ICRA), 2016, pp. 3006–3012. doi:10.1109/ICRA.2016.7487466.

[49] J. Liang, Q. Fei, B. Wang, Q. Geng, Tailsitter VTOL flying wing aircraft attitude control, in: 2016 31st Youth Academic Annual Conference of Chinese Association of Automation (YAC), 2016, pp. 439–443. doi:10.1109/YAC.2016.7804934.

[50] S. Verling, T. Stastny, G. Bättig, K. Alexis, R. Siegwart, Model-based transition optimization for a VTOL tailsitter, in: 2017 IEEE International Conference on Robotics and Automation (ICRA), 2017, pp. 3939–3944. doi:10.1109/ICRA.2017.7989454.

[51] S. Zhang, Q. Fei, J. Liang, Q. Geng, Modeling and control for longitudinal attitude of a twin-rotor tail-sitter unmanned aerial vehicle, in: 2017 13th IEEE International Conference on Control Automation (ICCA), 2017, pp. 816–821. doi:10.1109/ICCA.2017.8003165.

[52] L. Zhang, Z. Li, H. Liu, C. Wang, Robust attitude control for a tail-sitter aircraft, in: 2017 36th Chinese Control Conference (CCC), 2017, pp. 4900–4905. doi:10.23919/ChiCC.2017.8028128.

[53] R. Ritz, R. D'Andrea, A global controller for flying wing tailsitter vehicles, in: 2017 IEEE International Conference on Robotics and Automation (ICRA), 2017, pp. 2731–2738. doi:10.1109/ICRA.2017.7989318.

[54] R. Ritz, Enhancing the capabilities of flying machines: cooperative payload carrying, onboard learning, and tailsitter control, Ph.D. thesis, Swiss Federal Institute of Technology (ETH) Zurich (2017).

[55] J. M. O. Barth, J. Condomines, M. Bronz, L. R. Lustosa, J. Moschetta, C. Join, M. Fliess, Fixed-wing uav with transitioning flight capabilities : Model-based or model-free control approach? a preliminary study, in: 2018 International Conference on Unmanned Aircraft Systems (ICUAS), 2018, pp. 1157–1164. doi:10.1109/ICUAS.2018.8453404.

[56] R. Chiappinelli, M. Nahon, Modeling and control of a tailsitter UAV, in: 2018 International Conference on Unmanned Aircraft Systems (ICUAS), 2018, pp. 400–409. doi:10.1109/ICUAS.2018.8453301.

[57] Y. Yang, J. Zhu, X. Zhang, X. Wang, Active disturbance rejection control of a flying-wing tailsitter in hover flight, in: 2018 IEEE/RSJ International Conference on Intelligent Robots and Systems (IROS), 2018, pp. 6390–6396. doi:10.1109/IROS.2018.8594470.

[58] J. Zhong, B. Song, Y. Li, J. Xuan, L_1 adaptive control of a dual-rotor tail-sitter unmanned aerial vehicle with input constraints during hover flight, IEEE Access 7 (2019) 51312–51328. doi:10.1109/ACCESS.2019.2911897.

[59] J. M. O. Barth, J. Condomines, J. Moschetta, A. Cabarbaye, C. Join, M. Fliess, Full model-free control architecture for hybrid uavs, in: 2019 American Control Conference (ACC), 2019, pp. 71–78. doi:{10.23919/ACC.2019.8814993}.

[60] S. Fuhrer, S. Verling, T. Stastny, R. Siegwart, Fault-tolerant flight control of a VTOL tailsitter UAV, in: 2019 International Conference on Robotics and Automation (ICRA), 2019, pp. 4134–4140. doi:10.1109/ICRA.2019.8793467.

[61] J. Escareño, R. H. Stone, A. Sanchez, R. Lozano, Modeling and control strategy for the transition of a convertible tail-sitter UAV, in: 2007 European Control Conference (ECC), 2007, pp. 3385–3390. doi:10.23919/ECC.2007.7068919.

[62] J. Escareno, S. Salazar, R. Lozano, Modelling and control of a convertible VTOL aircraft, in: Proceedings of the 45th IEEE Conference on Decision and Control, 2006, pp. 69–74. doi:10.1109/CDC.2006.376915.

[63] J. Escareño, S. Salazar-Cruz, R. Lozano, Attitude stabilization of a convertible mini birotor, in: 2006 IEEE Conference on Computer Aided Control System Design, 2006 IEEE International Conference on Control Applications, 2006 IEEE

International Symposium on Intelligent Control, 2006, pp. 2202–2206. doi:10.1109/CACSD-CCA-ISIC.2006.4776982.

[64] R. H. Stone, Control architecture for a tail-sitter unmanned air vehicle, in: 2004 5th Asian Control Conference (IEEE Cat. No.04EX904), Vol. 2, 2004, pp. 736–744.

[65] O. Garcia, J. Escareno, V. Rosas, Unmanned Aerial Vehicles: Embedded Control, Wiley, 2010, Ch. 5, pp. 79–114.

[66] D. A. Ta, I. Fantoni, R. Lozano, Modeling and control of a convertible mini-UAV, IFAC Proceedings Volumes 44 (1) (2011) 1492–1497, 18th IFAC World Congress. doi:https://doi.org/10.3182/20110828-6-IT-1002.01066.
URL http://www.sciencedirect.com/science/article/pii/S1474667016438206

[67] P. Casau, D. Cabecinhas, C. Silvestre, Autonomous transition flight for a vertical take-off and landing aircraft, in: 2011 50th IEEE Conference on Decision and Control and European Control Conference, 2011, pp. 3974–3979. doi:10.1109/CDC.2011.6160819.

[68] P. Casau, D. Cabecinhas, C. Silvestre, Hybrid control strategy for the autonomous transition flight of a fixed-wing aircraft, IEEE Transactions on Control Systems Technology 21 (6) (2013) 2194–2211. doi:10.1109/TCST.2012.2221091.

[69] Y. Ke, B. M. Chen, Full envelope dynamics modeling and simulation for tail-sitter hybrid UAVs, in: 2017 36th Chinese Control Conference (CCC), 2017, pp. 2242–2247. doi:10.23919/ChiCC.2017.8027691.

[70] Y. Ke, K. Wang, K. Gong, S. Lai, B. M. Chen, Model based robust forward transition control for tail-sitter hybrid unmanned aerial vehicles, in: 2017 13th IEEE International Conference on Control Automation (ICCA), 2017, pp. 828–833. doi:10.1109/ICCA.2017.8003167.

[71] Y. Ke, K. Wang, B. M. Chen, Design and implementation of a hybrid UAV with model-based flight capabilities, IEEE/ASME Transactions on Mechatronics 23 (3) (2018) 1114–1125. doi:10.1109/TMECH.2018.2820222.

[72] X. Lyu, H. Gu, J. Zhou, Z. Li, S. Shen, F. Zhang, A hierarchical control approach for a quadrotor tail-sitter VTOL UAV and experimental verification, in: 2017 IEEE/RSJ International Conference on Intelligent Robots and Systems (IROS), 2017, pp. 5135–5141. doi:10.1109/IROS.2017.8206400.

[73] X. Lyu, H. Gu, Y. Wang, Z. Li, S. Shen, F. Zhang, Design and implementation of a quadrotor tail-sitter VTOL UAV, in: 2017 IEEE International Conference on Robotics and Automation (ICRA), 2017, pp. 3924–3930. doi:10.1109/ICRA.2017.7989452.

[74] X. Lyu, J. Zhou, H. Gu, Z. Li, S. Shen, F. Zhang, Disturbance observer based hovering control of quadrotor tail-sitter VTOL UAVs using H_∞ synthesis, IEEE Robotics and Automation Letters 3 (4) (2018) 2910–2917. doi:10.1109/LRA.2018.2847405.

[75] A. Flores, A. M. de Oca, G. Flores, A simple controller for the transition maneuver of a tail-sitter drone, CoRR abs/1810.11534 (2018). arXiv:1810.11534.
URL http://arxiv.org/abs/1810.11534

[76] A. Oosedo, S. Abiko, A. Konno, T. Koizumi, T. Furui, M. Uchiyama, Development of a quad rotor tail-sitter VTOL UAV without control surfaces and experimental verification, in: 2013 IEEE International Conference on Robotics and Automation, 2013, pp. 317–322. doi:10.1109/ICRA.2013.6630594.

[77] M. Hochstenbach, C. Notteboom, B. Theys, J. D. Schutter, Design and control of an unmanned aerial vehicle for autonomous parcel delivery with transition from vertical take-off to forward flight – vertikul, a quadcopter tailsitter, International Journal of Micro Air Vehicles 7 (4) (2015) 395–405. arXiv:https://doi.org/10.1260/1756-8293.7.4.395, doi:10.1260/1756-8293.7.4.395.
URL https://doi.org/10.1260/1756-8293.7.4.395

[78] B. Theys, G. De Vos, J. De Schutter, A control approach for transitioning VTOL UAVs with continuously varying transition angle and controlled by differential thrust, in: 2016 International Conference on Unmanned Aircraft Systems (ICUAS), 2016, pp. 118–125. doi:10.1109/ICUAS.2016.7502519.

[79] B. Theys, Phd thesis : Design methodology and control strategy for transitioning vertical takeoff and landing unmanned aerial vehicles for improved speed, range and payload capacity, Ph.D. thesis (2016).
URL https://lirias.kuleuven.be/retrieve/416508

[80] J. Zhou, X. Lyu, Z. Li, S. Shen, F. Zhang, A unified control method for quadrotor tail-sitter UAVs in all flight modes: hover, transition, and level flight, in: 2017 IEEE/RSJ International Conference on Intelligent Robots and Systems (IROS), 2017, pp. 4835–4841. doi:10.1109/IROS.2017.8206359.

[81] X. Zhao, H. Zhao, X. Wang, J. Yin, Modeling and hover attitude control of tail-sitter aircraft, in: 2018 33rd Youth Academic Annual Conference of Chinese Association of Automation (YAC), 2018, pp. 1017–1022. doi:10.1109/YAC.2018.8406520.

[82] Z. Li, W. Zhou, H. Liu, L. Zhang, Z. Zuo, Nonlinear robust flight mode transition control for tail-sitter aircraft, IEEE Access 6 (2018) 65909–65921. doi:10.1109/ACCESS.2018.2878722.

[83] Z. Li, W. Zhou, H. Liu, Robust controller design for a tail-sitter UAV in flight mode transitions, in: 2018 IEEE 14th International Conference on Control and Automation (ICCA), 2018, pp. 763–768. doi:10.1109/ICCA.2018.8444168.

[84] W. Xu, H. Gu, Y. Qing, J. Lin, F. Zhang, Full attitude control of an efficient quadrotor tail-sitter VTOL UAV with flexible modes, CoRR abs/1903.06393 (2019). arXiv:1903.06393.
URL http://arxiv.org/abs/1903.06393

[85] R. Gill, R. D'Andrea, An annular wing vtol uav: Flight dynamics and control, Drones 4 (2020) 14. doi:10.3390/drones4020014.

[86] B. Li, J. Sun, W. Zhou, C. Y. Wen, K. H. Low, C. K. Chen, Transition optimization for a vtol tail-sitter uav, IEEE/ASME Transactions on Mechatronics 25 (5) (2020) 2534–2545. doi:10.1109/TMECH.2020.2983255.

[87] Y. Wang, J. Yu, Q. Li, Z. Ren, Control strategy for the transition flight of a tail-sitter UAV, in: 2017 36th Chinese Control Conference (CCC), 2017, pp. 3504–3509. doi:10.23919/ChiCC.2017.8027900.

[88] Y. Wang, X. Lyu, H. Gu, S. Shen, Z. Li, F. Zhang, Design, implementation and verification of a quadrotor tail-sitter VTOL UAV, in: 2017 International Conference on Unmanned Aircraft Systems (ICUAS), 2017, pp. 462–471. doi:10.1109/ICUAS.2017.7991419.

[89] N. Raj, A. Simha, M. Kothari, Abhishek, R. N. Banavar, Iterative Learning Based Feedforward Control for Transition of a Biplane-Quadrotor Tailsitter UAS, in: 2020 IEEE International Conference on Robotics and Automation (ICRA), 2020, pp. 321–327. doi:10.1109/ICRA40945.2020.9196671.

[90] J. Xu, T. Du, M. Foshey, B. Li, B. Zhu, A. Schulz, W. Matusik, Learning to fly: computational controller design for hybrid uavs with reinforcement learning, ACM Transactions on Graphics 38 (2019) 1–12. doi:10.1145/3306346.3322940.

[91] L. Deyuan, L. Hao, L. Zhaoying, Robust mode transition attitude control of tail-sitter unmanned aerial vehicles, in: 2017 36th Chinese Control Conference (CCC), 2017, pp. 3198–3202. doi:10.23919/ChiCC.2017.8027849.

[92] D. Liu, H. Liu, C. Liu, B. Zhu, Z. Li, Robust optimal attitude controller design for tail-sitters, in: 2018 Annual American Control Conference (ACC), 2018, pp. 4233–4237. doi:10.23919/ACC.2018.8431535.

[93] D. Liu, H. Liu, F. L. Lewis, K. P. Valavanis, Robust time-varying formation control for tail-sitters in flight mode transitions, IEEE Transactions on Systems, Man, and Cybernetics: Systems (2019) 1–10doi:10.1109/TSMC.2019.2931482.

[94] H. Liu, F. Peng, F. L. Lewis, Y. Wan, Robust tracking control for tail-sitters in flight mode transitions, IEEE Transactions on Aerospace and Electronic Systems 55 (4) (2019) 2023–2035. doi:10.1109/TAES.2018.2880888.

[95] L. Deyuan, L. Hao, L. Zhaoying, Z. Wanbing, Robust trajectory tracking control for tail-sitter UAVs, in: 2018 37th Chinese Control Conference (CCC), 2018, pp. 2538–2542. doi:10.23919/ChiCC.2018.8483277.

[96] R. T. Rysdyk, A. J. Calise, Adaptive model inversion flight control for tilt-rotor aircraft, Journal of Guidance, Control, and Dynamics 22 (3) (1999) 402–407. arXiv:https://doi.org/10.2514/2.4411, doi:10.2514/2.4411.
URL https://doi.org/10.2514/2.4411

[97] R. T. Rysdyk, A. J. Calise, Adaptive nonlinear control for tiltrotor aircraft, in: Proceedings of the 1998 IEEE International Conference on Control Applications (Cat. No.98CH36104), Vol. 2, 1998, pp. 980–984. doi:10.1109/CCA.1998.721604.

[98] R. K. Mehra, R. K. Prasanth, S. Gopalaswamy, XV-15 tiltrotor flight control system design using model predictive control, in: 1998 IEEE Aerospace Conference Proceedings (Cat. No.98TH8339), Vol. 2, 1998, pp. 139–148. doi:10.1109/AERO.1998.687905.

[99] Jang-Ho Lee, Byoung-Mun Min, Eung-Tai Kim, Autopilot design of tilt-rotor UAV using particle swarm optimization method, in: 2007 International Conference on Control, Automation and Systems, 2007, pp. 1629–1633. doi:10.1109/ICCAS.2007.4406594.

[100] S. Yanguo, W. Huanjin, Design of flight control system for a small unmanned tilt rotor aircraft, Chinese Journal of Aeronautics 22 (3) (2009) 250–256. doi:https://doi.org/10.1016/S1000-9361(08)60095-3.
URL http://www.sciencedirect.com/science/article/pii/S1000936108600953

[101] Chih-Cheng Peng, Thong-Shing Hwang, Shiaw-Wu Chen, Ching-Yi Chang, Yi-Ciao Lin, Yao-Ting Wu, Yi-Jing Lin, Wei-Ren Lai, ZPETC path-tracking gain-scheduling design and real-time multi-task flight simulation for the automatic transition of tilt-rotor aircraft, in: 2010 IEEE Conference on Robotics, Automation and Mechatronics, 2010, pp. 118–123. doi:10.1109/RAMECH.2010.5513203.

[102] B.-M. Kim, B. Kim, N. Kim, Trajectory tracking controller design using neural networks for a tiltrotor unmanned aerial vehicle, Proceedings of The Institution of Mechanical Engineers Part G-journal of Aerospace Engineering - PROC INST

MECH ENG G-J A E 224 (2010) 881–896. doi:10.1243/09544100JAERO710.

[103] J. T. VanderMey, A tilt rotor UAV for long endurance operations in remote environments, Master's thesis, Massachusetts Institute of Technology (2011).
URL https://dspace.mit.edu/handle/1721.1/67196

[104] X. Fang, Q. Lin, Y. Wang, L. Zheng, Control strategy design for the transitional mode of tiltrotor UAV, in: IEEE 10th International Conference on Industrial Informatics, 2012, pp. 248–253. doi:10.1109/INDIN.2012.6300840.

[105] S. Park, J. Bae, Y. Kim, S. Kim, Fault tolerant flight control system for the tilt-rotor UAV, Journal of the Franklin Institute 350 (9) (2013) 2535–2559. doi:https://doi.org/10.1016/j.jfranklin.2013.01.014.
URL http://www.sciencedirect.com/science/article/pii/S0016003213000318

[106] R. G. Hernández-García, H. Rodríguez-Cortés, Transition flight control of a cyclic tiltrotor UAV based on the gain-scheduling strategy, in: 2015 International Conference on Unmanned Aircraft Systems (ICUAS), 2015, pp. 951–956. doi:10.1109/ICUAS.2015.7152383.

[107] S. Song, W. Wang, K. Lu, L. Sun, Nonlinear attitude control using extended state observer for tilt-rotor aircraft, in: The 27th Chinese Control and Decision Conference (2015 CCDC), 2015, pp. 852–857. doi:10.1109/CCDC.2015.7162038.

[108] K. Lu, C. Liu, Z. Wang, W. Wang, Modeling and control of tilt-rotor aircraft, in: 2016 Chinese Control and Decision Conference (CCDC), 2016, pp. 550–553. doi:10.1109/CCDC.2016.7531046.

[109] H. Lin, R. Fu, J. Zeng, Extended state observer based sliding mode control for a tilt rotor UAV, in: 2017 36th Chinese Control Conference (CCC), 2017, pp. 3771–3775. doi:10.23919/ChiCC.2017.8027947.

[110] Z. Pan, C. Chi, J. Zhang, Nonlinear attitude control of tiltrotor aircraft in helicopter mode based on ADRSM theory, in: 2018 37th Chinese Control Conference (CCC), 2018, pp. 9962–9967. doi:10.23919/ChiCC.2018.8483589.

[111] D. N. Cardoso, S. Esteban, G. V. Raffo, A nonlinear W_∞ controller of a tilt-rotor UAV for trajectory tracking, in: 2019 18th European Control Conference (ECC), 2019, pp. 928–934. doi:10.23919/ECC.2019.8795894.

[112] Y. Kang, N. Kim, B. Kim, M.-J. Tahk, Autopilot design for tilt-rotor unmanned aerial vehicle with nacelle mounted wing extension using single hidden layer perceptron neural network, Proceedings of the Institution of Mechanical Engineers, Part G: Journal of Aerospace Engineering 231 (08 2016). doi:10.1177/0954410016664926.

[113] D. A. Ta, I. Fantoni, R. Lozano, Modeling and control of a tilt tri-rotor airplane, in: 2012 American Control Conference (ACC), 2012, pp. 131–136. doi:10.1109/ACC.2012.6315155.

[114] A. S. Onen, L. Cevher, M. Senipek, T. Mutlu, O. Gungor, I. O. Uzunlar, D. F. Kurtulus, O. Tekinalp, Modeling and controller design of a VTOL UAV, in: 2015 International Conference on Unmanned Aircraft Systems (ICUAS), 2015, pp. 329–337. doi:10.1109/ICUAS.2015.7152307.

[115] C. Chao, S. Lincheng, Z. Daibing, Z. Jiyang, Mathematical modeling and control of a tiltrotor UAV, in: 2016 IEEE International Conference on Information and Automation (ICIA), 2016, pp. 2016–2021. doi:10.1109/ICInfA.2016.7832150.

[116] L. Yu, D. Zhang, J. Zhang, C. Pan, Modeling and attitude control of a tilt tri-rotor UAV, in: 2017 36th Chinese Control Conference (CCC), 2017, pp. 1103–1108. doi:10.23919/ChiCC.2017.8027494.

[117] L. Yu, D. Zhang, J. Zhang, Transition flight modeling and control of a novel tilt tri-rotor UAV, in: 2017 IEEE International Conference on Information and Automation (ICIA), 2017, pp. 983–988. doi:10.1109/ICInfA.2017.8079045.

[118] J. A. Bautista, A. Osorio, R. Lozano, Modeling and analysis of a tricopter/flying-wing convertible UAV with tilt-rotors, in: 2017 International Conference on Unmanned Aircraft Systems (ICUAS), 2017, pp. 672–681. doi:10.1109/ICUAS.2017.7991502.

[119] M. Umer, S. M. A. Kazmi, S. M. H. Askari, D. I. A. Rana, Design and modeling of VTOL tri tilt-rotor aircraft, in: 2018 15th International Conference on Smart Cities: Improving Quality of Life Using ICT IoT (HONET-ICT), 2018, pp. 1–5. doi:10.1109/HONET.2018.8551474.

[120] D. Yangping, G. Honggang, Transition flight control and test of a new kind tilt prop box-wing VTOL UAV, in: 2018 9th International Conference on Mechanical and Aerospace Engineering (ICMAE), 2018, pp. 90–94. doi:10.1109/ICMAE.2018.8467657.

[121] L. Yu, G. He, S. Zhao, X. Wang, Dynamic inversion-based sliding mode control of a tilt tri-rotor UAV, in: 2019 12th Asian Control Conference (ASCC), 2019, pp. 1637–1642.

[122] N. T. Hegde, V. I. George, C. G. Nayak, Modelling and transition flight control of vertical take-off and landing unmanned tri-tilting rotor aerial vehicle, in: 2019 3rd International conference on Electronics, Communication and Aerospace Technology (ICECA), 2019, pp. 590–594. doi:10.1109/ICECA.2019.8821804.

[123] S. Chang, A. Cho, S. Choi, Y. Kang, Y. Kim, M. Kim, Flight testing full conversion of a 40-kg-class tilt-duct unmanned aerial

vehicle, Aerospace Science and Technology 112 (2021) 106611. doi:https://doi.org/10.1016/j.ast.2021.106611.
URL https://www.sciencedirect.com/science/article/pii/S1270963821001218

[124] J. Tavoosi, Hybrid intelligent adaptive controller for tiltrotor uav, International Journal of Intelligent Unamnned Systems (August 2020).

[125] E. D´Amato, G. Francesco, I. Notaro, G. Tartaglione, M. Mattei, Nonlinear Dynamic Inversion and Neural Networks for a Tilt Tri-Rotor UAV, IFAC-PapersOnLine 48 (2015) 162–167. doi:10.1016/j.ifacol.2015.08.077.

[126] C. Papachristos, K. Alexis, A. Tzes, Towards a high-end unmanned tri-tiltrotor: design, modeling and hover control, in: 2012 20th Mediterranean Conference on Control Automation (MED), 2012, pp. 1579–1584. doi:10.1109/MED.2012.6265864.

[127] C. Papachristos, A. Tzes, Modeling and control simulation of an unmanned tilt tri-rotor aerial vehicle, in: 2012 IEEE International Conference on Industrial Technology, 2012, pp. 840–845. doi:10.1109/ICIT.2012.6210043.

[128] C. Papachristos, K. Alexis, A. Tzes, Linear quadratic optimal position control for an unmanned tri-tiltrotor, in: 2013 International Conference on Control, Decision and Information Technologies (CoDIT), 2013, pp. 708–713. doi:10.1109/CoDIT.2013.6689629.

[129] C. Papachristos, K. Alexis, A. Tzes, Model predictive hovering-translation control of an unmanned tri-tiltrotor, in: 2013 IEEE International Conference on Robotics and Automation, 2013, pp. 5425–5432. doi:10.1109/ICRA.2013.6631355.

[130] S. Verling, J. Zilly, Modeling and control of a VTOL glider, Master's thesis, Swiss Federal Institute of Technology Zurich (2013).
URL https://docplayer.net/23088463-Modeling-and-control-of-a-vtol-glider.html

[131] G. R. Flores Colunga, J. A. Escareño, R. Lozano, S. Salazar, Four tilting rotor convertible MAV: Modeling and real-time hover flight control, Journal of Intelligent and Robotic Systems 65 (1-4) (2012) 457–471. doi:10.1007/s10846-011-9589-x.
URL https://hal.archives-ouvertes.fr/hal-00923129

[132] G. Flores, J. Escareno, R. Lozano, S. Salazar, Quad-tilting rotor convertible MAV: modeling and real-time hover flight control, Journal of Intelligent and Robotic Systems 65 (2012) 457–471. doi:10.1007/s10846-011-9589-x.

[133] G. Flores, R. Lozano, Transition flight control of the quad-tilting rotor convertible MAV, in: 2013 International Conference on Unmanned Aircraft Systems (ICUAS), 2013, pp. 789–794. doi:10.1109/ICUAS.2013.6564761.

[134] G. Ducard, M. Hua, Modeling of an unmanned hybrid aerial vehicle, in: Proceedings of the IEEE Multi-Conference on Systems and Control, Invited Session on UAVs, Antibes, France, 2014. doi:10.1109/CCA.2014.6981467.

[135] Q. Lin, Z. Cai, J. Yang, Y. Sang, Y. Wang, Trajectory tracking control for hovering and acceleration maneuver of quad tilt rotor UAV, in: Proceedings of the 33rd Chinese Control Conference, 2014, pp. 2052–2057. doi:10.1109/ChiCC.2014.6896946.

[136] G. Flores, I. Lugo, R. Lozano, 6-DOF hovering controller design of the quad tiltrotor aircraft: Simulations and experiments, in: 53rd IEEE Conference on Decision and Control, 2014, pp. 6123–6128. doi:10.1109/CDC.2014.7040348.

[137] G. R. Flores-Colunga, R. Lozano-Leal, A nonlinear control law for hover to level flight for the quad tilt-rotor UAV, IFAC Proceedings Volumes 47 (3) (2014) 11055–11059, 19th IFAC World Congress. doi:https://doi.org/10.3182/20140824-6-ZA-1003.02708.
URL http://www.sciencedirect.com/science/article/pii/S1474667016433720

[138] E. Cetinsoy, Design and control of a gas-electric hybrid quad tilt-rotor UAV with morphing wing, in: 2015 International Conference on Unmanned Aircraft Systems (ICUAS), 2015, pp. 82–91. doi:10.1109/ICUAS.2015.7152278.

[139] C. Chen, L. Shen, D. Zhang, J. Zhang, Identification and control of a hovering tiltrotor UAV, in: 2016 12th World Congress on Intelligent Control and Automation (WCICA), 2016, pp. 2226–2231. doi:10.1109/WCICA.2016.7578432.

[140] Z. Liu, D. Theilliol, L. Yang, Y. He, J. Han, Transition control of tilt rotor unmanned aerial vehicle based on multi-model adaptive method, in: 2017 International Conference on Unmanned Aircraft Systems (ICUAS), 2017, pp. 560–566. doi:10.1109/ICUAS.2017.7991339.

[141] Z. Liu, D. Theilliol, L. Yang, Y. He, J. Han, Observer-based linear parameter varying control design with unmeasurable varying parameters under sensor faults for quad-tilt rotor unmanned aerial vehicle, Aerospace Science and Technology 92 (2019) 696–713. doi:https://doi.org/10.1016/j.ast.2019.06.028.
URL http://www.sciencedirect.com/science/article/pii/S1270963818321722

[142] A. Anglade, J.-M. Kai, T. Hamel, C. Samson, Automatic control of convertible fixed-wing drones with vectorized thrust, Research report, INRIA Sophia Antipolis - I3S (Apr. 2019).
URL https://hal.archives-ouvertes.fr/hal-02111045

[143] M. Allenspach, G. J. J. Ducard, Model predictive control of a convertible tiltrotor unmanned aerial vehicle, in: 2020 28th Mediterranean Conference on Control and Automation (MED), 2020, pp. 715–720. doi:10.1109/MED48518.2020.9183353.

[144] L. Bauersfeld, G. Ducard, Fused-pid control for tilt-rotor vtol aircraft, in: 2020 28th Mediterranean Conference on Control and Automation (MED), 2020, pp. 703–708. doi:10.1109/MED48518.2020.9183031.

[145] L. Spannagl, G. Ducard, Control allocation for an unmanned hybrid aerial vehicle, in: 2020 28th Mediterranean Conference on Control and Automation (MED), 2020, pp. 709–714. doi:10.1109/MED48518.2020.9182865.

[146] M. Allenspach, G. J. J. Ducard, Nonlinear model predictive control and guidance for a propeller-tilting hybrid unmanned air vehicle, Automatica 132 (2021) 109790. doi:https://doi.org/10.1016/j.automatica.2021.109790.
URL https://www.sciencedirect.com/science/article/pii/S0005109821003101

[147] L. Bauersfeld, L. Spannagl, G. Ducard, C. Onder, MPC Flight Control for a Tilt-rotor VTOL Aircraft, IEEE Transactions on Aerospace and Electronic Systems (2021). doi:10.1109/TAES.2021.3061819.

[148] B. Li, W. Zhou, J. Sun, C.-Y. Wen, C.-K. Chen, Development of model predictive controller for a tail-sitter vtol uav in hover flight, Sensors 18 (9) (2018) 2859. doi:10.3390/s18092859.
URL http://dx.doi.org/10.3390/s18092859

[149] D. Shen, Q. Lu, M. Hu, Z. Kong, Mathematical modeling and control of the quad tilt-rotor UAV, in: 2018 IEEE 8th Annual International Conference on CYBER Technology in Automation, Control, and Intelligent Systems (CYBER), 2018, pp. 1220–1225. doi:10.1109/CYBER.2018.8688053.

[150] Y. Yin, H. Niu, X. Liu, Adaptive neural network sliding mode control for quad tilt rotor aircraft, Complexity 2017 (2017) 1–13. doi:10.1155/2017/7104708.

[151] T. Ostermann, J. Holsten, Y. Dobrev, D. Moormann, Control Concept of a Tiltwing UAV During Low Speed Manoeuvring, in: 28th International Congress of the Aeronautical Scienes : ICAS2012 ; 23. - 28. Sept. 2012, Brisbane, Australien, Optimage Ltd., Edinburgh, UK, 2012, 1 CD-ROM.
URL http://publications.rwth-aachen.de/record/97342

[152] E. Small, E. Fresk, G. Andrikopoulos, G. Nikolakopoulos, Modelling and control of a tilt-wing unmanned aerial vehicle, in: 2016 24th Mediterranean Conference on Control and Automation (MED), 2016, pp. 1254–1259. doi:10.1109/MED.2016.7536050.

[153] P. Hartmann, Predictive flight path control for tilt-wing aircraft, Ph.d. dissertation, Rheinisch-Westfällische Technische Hochschule Aachen (Nov. 2017).

[154] D. Rohr, T. Stastny, S. Verling, R. Siegwart, Attitude- and cruise control of a VTOL tiltwing UAV, IEEE Robotics and Automation Letters 4 (3) (2019) 2683–2690. arXiv:1903.10623v2, doi:10.1109/LRA.2019.2914340.

[155] D. Rohr, M. Studiger, T. Stastny, N. R. J. Lawrance, R. Siegwart, Nonlinear model predictive velocity control of a vtol tiltwing uav, IEEE Robotics and Automation Letters 6 (3) (2021) 5776–5783. doi:10.1109/LRA.2021.3084888.

[156] J. Autenrieb, H.-S. Shin, M. Bacic, Development of a neural network-based adaptive nonlinear dynamic inversion controller for a tilt-wing vtol aircraft, 2019, pp. 44–52. doi:10.1109/REDUAS47371.2019.8999700.

[157] K. T. Oner, E. Cetinsoy, M. Unel, M. F. Aksit, I. Kandemir, K. Gulez, Dynamic model and control of a new quadrotor unmanned aerial vehicle with tilt-wing mechanism, International Journal of Aerospace and Mechanical Engineering 2 (9) (2008) 1008–1013.
URL https://publications.waset.org/vol/21

[158] K. Muraoka, N. Okada, D. Kubo, Quad tilt wing VTOL UAV: Aerodynamic characteristics and prototype flight test, in: AIAA Infotech@Aerospace Conference, 2009. doi:https://doi.org/10.2514/6.2009-1834.

[159] S. Suzuki, R. ZHijia, Y. Horita, K. Nonami, G. Kimura, T. Bando, D. Hirabayashi, M. Furuya, K. Yasuda, Attitude control of quad rotors QTW-UAV with tilt wing mechanism, Journal of System Design and Dynamics 4 (3) (2010) 416–428. doi:10.1299/jsdd.4.416.

[160] C. Hancer, K. T. Oner, E. Sirimoglu, E. Cetinsoy, M. Unel, Robust hovering control of a quad tilt-wing UAV, in: IECON 2010 - 36th Annual Conference on IEEE Industrial Electronics Society, 2010, pp. 1615–1620. doi:10.1109/IECON.2010.5675441.

[161] C. Hancer, K. T. Oner, E. Sirimoglu, E. Cetinsoy, M. Unel, Robust position control of a tilt-wing quadrotor, in: 49th IEEE Conference on Decision and Control (CDC), 2010, pp. 4908–4913. doi:10.1109/CDC.2010.5717283.

[162] K. T. Oner, E. Cetinsoy, E. Sirimoglu, C. Hancer, T. Ayken, M. Unel, LQR and SMC stabilization of a new unmanned aerial vehicle, International Journal of Aerospace and Mechanical Engineering 3 (10) (2009) 1190–1195.

URL https://publications.waset.org/vol/34

[163] K. Muraoka, N. Okada, D. Kubo, M. Sato, Transition flight of quad tilt wing VTOL UAV, in: 28th International Congress of the Aeronautical Sciences, 2012.

[164] K. Oner, E. Cetinsoy, E. Cetinsoy, E. Sirimoglu, E. Sirimoglu, C. Hançer, C. Hancer, M. Ünel, M. Unel, M. Akşit, M. Aksit, K. Gülez, K. Gulez, I. Kandemir, Mathematical modeling and vertical flight control of a tilt-wing UAV, Turkish Journal of Electrical Engineering and Computer Sciences 20 (2012) 149–157. doi:10.3906/elk-1007-624.

[165] E. Cetinsoy, S. Dikyar, C. Hancer, K. Oner, E. Sirimoglu, M. Unel, M. Aksit, Design and construction of a novel quad tilt-wing UAV, Mechatronics 22 (2012) 723–745. doi:10.1016/j.mechatronics.2012.03.003.

[166] T. Mikami, K. Uchiyama, Design of flight control system for quad tilt-wing UAV, in: 2015 International Conference on Unmanned Aircraft Systems (ICUAS), 2015, pp. 801–805. doi:10.1109/ICUAS.2015.7152364.

[167] Y. Yildiz, M. Unel, A. E. Demirel, Adaptive nonlinear hierarchical control of a quad tilt-wing UAV, in: 2015 European Control Conference (ECC), 2015, pp. 3623–3628. doi:10.1109/ECC.2015.7331093.

[168] K. Benkhoud, S. Bouallègue, Model predictive control design for a convertible quad tilt-wing UAV, in: 2016 4th International Conference on Control Engineering Information Technology (CEIT), 2016, pp. 1–6. doi:10.1109/CEIT.2016.7929042.

[169] K. Benkhoud, S. Bouallègue, Modeling and LQG controller design for a quad tilt-wing UAV, in: 3rd International Conference on Automation, Control, Engineering and Computer Science, 2016.

[170] K. Benkhoud, S. Bouallègue, M. Ayadi, Rapid control prototyping of a quad-tilt-wing unmanned aerial vehicle, in: 2017 International Conference on Control, Automation and Diagnosis (ICCAD), 2017, pp. 423–428. doi:10.1109/CADIAG.2017.8075696.

[171] S. Panza, M. Sato, M. Lovera, K. Muraoka, Robust attitude control design of quad-tilt-wing UAV: a structured μ-synthesis approach, in: IEEE Conference on Control Technology and Applications, 2018. doi:10.1109/CCTA.2018.8511407.

[172] D. Mix, J. Koenig, K. Linda, O. Cifdaloz, V. Wells, A. Rodriguez, Towards gain-scheduled H_∞ control design for a tilt-wing aircraft, in: Proceedings of the IEEE Conference on Decision and Control, Vol. 2, 2004, pp. 1222–1227. doi:10.1109/CDC.2004.1430208.

[173] J. J. Dickeson, D. R. Mix, J. S. Koenig, K. M. Linda, O. Cifdaloz, V. L. Wells, A. A. Rodriguez, H_∞ hover-to-cruise conversion for a tilt-wing rotorcraft, in: Proceedings of the 44th IEEE Conference on Decision and Control, 2005, pp. 6486–6491. doi:10.1109/CDC.2005.1583202.

[174] J. J. Dickeson, O. Cifdaloz, D. W. Miles, P. M. Koziol, V. L. Wells, A. A. Rodriguez, Robust H_∞ gain-scheduled conversion for a tilt-wing rotorcraft, in: Proceedings of the 45th IEEE Conference on Decision and Control, 2006, pp. 5882–5887. doi:10.1109/CDC.2006.377256.

[175] J. Dickeson, D. Miles, O. Cifdaloz, V. Wells, A. Rodriguez, Robust LPV H_∞ gain-scheduled hover-to-cruise conversion for a tilt-wing rotorcraft in the presence of CG variations, in: Proceedings of the 46th IEEE Conference on Decision and Control, 2007, pp. 2773–2778. doi:10.1109/CDC.2007.4435028.

[176] A. S. Saeed, A. B. Younes, S. Islam, J. Dias, L. Seneviratne, G. Cai, A review on the platform design, dynamic modeling and control of hybrid UAVs, in: 2015 International Conference on Unmanned Aircraft Systems (ICUAS), 2015, pp. 806–815. doi:10.1109/ICUAS.2015.7152365.

[177] H. Yeo, W. Johnson, Performance and design investigation of heavy lift tilt-rotor with aerodynamic interference effects, Journal of Aircraft 46 (4) (2009) 1231 – 1239. doi:https://doi.org/10.2514/1.40102.

[178] L. Kingston, J. DeTore, Tilt rotor v/stol aircraft technology, in: Second European Rotorcraft and Powered Lift Aircraft Forum, 36, Deutsche Gesellschaft für Luft- und Raumfahrt e.V. Postfach 510645 D-5000 Köln Germany, Bückeburg, Germany, 1976, pp. 1 – 13.
URL https://dspace-erf.nlr.nl/xmlui/handle/20.500.11881/2041?show=full

[179] R. W. Prouty, Helicopter performance, stability, and control , PWS Engineering, 1986.

[180] S. Newman, The foundations of helicopter flight, Halsted Press, 2001.

[181] T. Hamel, R. Mahony, R. Lozano, J. Ostrowski, Dynamic modelling and configuration stabilization for an X4-flyer, in: IFAC World Congress, 2002, pp. 200–212. doi:10.3182/20020721-6-ES-1901.00848.

[182] S. Bouabdallah, Design and Control of Quadrotors with Application to Autonomous Flying, Ph.D. thesis, EPF Lausanne (2007).

[183] John H. Blakelock, Automatic Control of Aircraft and Missiles, 2nd Edition, Wiley, 1991.

[184] B. Stevens, F. Lewis, Aircraft Control and Simulation, Second Edition, Wiley, New York, NY, 2003.

[185] R. F. Stengel, Flight Dynamics, Princeton University Press, Princeton, New Jersey, 2004.

[186] M. Möckli, Guidance and Control for Aerobatic Maneuvers of an Unmanned Airplane, Ph.D. thesis, ETH Zürich, diss No. 16586 (2006).

[187] G. Ducard, Fault-tolerant Flight Control and Guidance Systems: Practical Methods for Small Unmanned Aerial Vehicles, Advances in Industrial Control, ISBN: 978-1-84882-560-4, Springer-Verlag London, 2009.
URL https://www.springer.com/gp/book/9781848825604

[188] R. W. Beard, T. W. McLain, Small Unmanned Aircraft: Theory and Practice, Princeton University Press, Princeton and Oxford, 2012.

[189] B. gang Mi, H. Zhan, S. si Lu, An extended unsteady aerodynamic model at high angles of attack, Aerospace Science and Technology 77 (2018) 788–801. doi:https://doi.org/10.1016/j.ast.2018.03.035.
URL https://www.sciencedirect.com/science/article/pii/S1270963817323933

[190] B. Yuksek, A. Vuruskan, U. Vuruskan, M. A. Yukselen, G. Inalhan, Transition flight modeling of a fixed-wing vtol uav, Journal of Intelligent and Robotic Systems 84 (2016) 83 – 105. doi:https://doi.org/10.1007/s10846-015-0325-9.

[191] Y. Govdeli, M. B. M. Sheikh, R. Raj, B. Elhadidi, E. Kayacan, Unsteady aerodynamic modeling and control of pusher and tilt-rotor quadplane configurations, Aerospace Science and Technology 94 (2019) 105421. doi:10.1016/j.ast.2019.105421.

[192] Dufour Aerospace, Tiltwing concept (2021).
URL https://dufour.aero/

[193] M. Tyan, N. V. Nguyen, S. Kim, J.-W. Lee, Comprehensive preliminary sizing/resizing method for a fixed wing – vtol electric uav, Aerospace Science and Technology 71 (2017) 30–41. doi:https://doi.org/10.1016/j.ast.2017.09.008.
URL https://www.sciencedirect.com/science/article/pii/S1270963817300871

[194] S. Darvishpoor, J. Roshanian, M. Tayefi, A novel concept of vtol bi-rotor uav based on moving mass control, Aerospace Science and Technology 107 (2020) 106238. doi:https://doi.org/10.1016/j.ast.2020.106238.
URL https://www.sciencedirect.com/science/article/pii/S1270963820309202

[195] C. Zeng, R. Abnous, K. Gabani, S. Chowdhury, V. Maldonado, A new tilt-arm transitioning unmanned aerial vehicle: Introduction and conceptual design, Aerospace Science and Technology 99 (2020) 105755. doi:https://doi.org/10.1016/j.ast.2020.105755.
URL https://www.sciencedirect.com/science/article/pii/S1270963819317961

[196] Y. Zhou, G. Huang, C. Xia, Analysis of fixed-wing vtol aircraft with gas-driven fan propulsion system, Aerospace Science and Technology 104 (2020) 105984. doi:https://doi.org/10.1016/j.ast.2020.105984.
URL https://www.sciencedirect.com/science/article/pii/S1270963820306660

[197] Özgür Dündar, M. Bilici, T. Ünler, Design and performance analyses of a fixed wing battery VTOL UAV, Engineering Science and Technology, an International Journal 23 (2020) 1182 – 1193. doi:https://doi.org/10.1016/j.jestch.2020.02.002.

[198] H. Zhang, B. Song, F. Li, J. Xuan, Multidisciplinary design optimization of an electric propulsion system of a hybrid uav considering wind disturbance rejection capability in the quadrotor mode, Aerospace Science and Technology 110 (2021) 106372. doi:https://doi.org/10.1016/j.ast.2020.106372.
URL https://www.sciencedirect.com/science/article/pii/S1270963820310543

[199] B. Theys, G. Dimitriadis, P. Hendrick, Experimental and numerical study of micro-aerial-vehicle propeller performance in oblique flow, Journal of Aircraft 54 (2016) 1–9. doi:10.2514/1.C033618.

[200] B. Theys, G. Dimitriadis, P. Hendrick, Influence of propeller configuration on propulsion system efficiency of multi-rotor unmanned aerial vehicles, 2016, pp. 195–201. doi:10.1109/ICUAS.2016.7502520.

[201] R. J. Higgins, G. N. Barakos, S. Shahpar, I. Tristanto, A computational fluid dynamic acoustic investigation of a tiltwing evtol concept aircraft, Aerospace Science and Technology 111 (2021) 106571. doi:https://doi.org/10.1016/j.ast.2021.106571.
URL https://www.sciencedirect.com/science/article/pii/S1270963821000821

[202] D. Phung, P. Morin, Modeling and energy evaluation of small convertible UAVs, in: 2nd Workshop on Research, Education and Development of Unmanned Aerial Systems, 2013.

[203] M. Blanke, M. Kinnaert, J. Lunze, M. Staroswiecki, Diagnosis and Fault Tolerant Control, Springer Verlag, London, 2006.

[204] B. Benini, P. Castaldi, S. Simani, Fault Diagnosis for Aircraft System Models: An Introduction from Fault Detection to Fault Tolerance, VDM Verlag Dr. Muller, Saarbrucken, 2009.

[205] H. Alwi, C. Edwards, C. P. Tan, Fault Detection and Fault Tolerant Control Using Sliding Modes, Springer-Verlag, 2011,

iSBN: 978-0-85729-649-8.

[206] G. Ducard, Actuator Fault Detection in UAVs, Springer-Verlag London, London, 2014, 48 pages.

[207] Z. Liu, Y. He, L. Yang, J. Han, Control techniques of tilt rotor unmanned aerial vehicle systems: A review, Chinese Journal of Aeronautics 30 (1) (2017) 135–148. doi:https://doi.org/10.1016/j.cja.2016.11.001.
URL http://www.sciencedirect.com/science/article/pii/S1000936116302199

[208] R. Naldi, L. Marconi, Optimal transition maneuvers for a class of V/STOL aircraft, Automatica 47 (5) (2011) 870–879. doi:https://doi.org/10.1016/j.automatica.2011.01.027.
URL http://www.sciencedirect.com/science/article/pii/S0005109811000422

[209] D. Kubo, S. Suzuki, Tail-sitter vertical takeoff and landing unmanned aerial vehicle: Transitional flight analysis, Journal of Aircraft 45 (1) (2008) 292–297. arXiv:https://doi.org/10.2514/1.30122, doi:10.2514/1.30122.
URL https://doi.org/10.2514/1.30122

[210] S. Omari, M.-D. Hua, G. Ducard, T. Hamel, Hardware and Software Architecture for Nonlinear Control of Multirotor Helicopters, IEEE Transactions on Mechatronics 18 (6) (2013) 1724–1736. doi:{10.1109/TMECH.2013.2274558}.

[211] J. Escareño, A. Sanchez, O. Garcia, R. Lozano, Modeling and global control of the longitudinal dynamics of a coaxial convertible mini-UAV in hover mode, Journal of Intelligent and Robotic Systems 54 (1-3) (2008) 261–273.

[212] S. Park, J. Deyst, J. P. How, Performance and Lyapunov Stability of a Nonlinear Path-Following Guidance Method, AIAA Journal of Guidance, Control, and Dynamics 30 (6) (2007) 1718–1728.

[213] K. Wang, Y. Ke, B. M. Chen, Development of autonomous hybrid UAV U-Lion with VTOL and cruise flying capabilities, in: 2016 IEEE International Conference on Advanced Intelligent Mechatronics (AIM), 2016, pp. 1053–1060. doi:10.1109/AIM.2016.7576909.

[214] G. Ducard, K. C. Kulling, H. P. Geering, A Simple and Adaptive On-Line Path Planning System for a UAV, in: Proceedings of the IEEE 15th Mediterranean Conference on Control and Automation, Athens, Greece, 2007, pp. 1–6, t34-009. doi:10.1109/MED.2007.4433931.

[215] A. Banazadeh, N. Assadian, F. Saghafi, Minimum time trajectory optimization of a tail-sitter aerial vehicle using nonlinear programming, in: The 2012 International Conference on Advanced Mechatronic Systems, 2012, pp. 275–280.

[216] V. Martinez, O. Garcia, A. Sanchez, V. Parra, A. Escobar, Adaptive backstepping control for a convertible UAV, in: 2015 Workshop on Research, Education and Development of Unmanned Aerial Systems (RED-UAS), 2015, pp. 298–307. doi:10.1109/RED-UAS.2015.7441020.

[217] P. Huangzhong, Z. Ziyang, G. Chen, Tiltrotor aircraft attitude control in conversion mode based on optimal preview control, in: Proceedings of 2014 IEEE Chinese Guidance, Navigation and Control Conference, 2014, pp. 1544–1548. doi:10.1109/CGNCC.2014.7007422.

[218] J. Sun, J. Yang, X. Zhu, Robust flight control law development for tiltrotor conversion, in: 2009 International Conference on Intelligent Human-Machine Systems and Cybernetics, Vol. 2, 2009, pp. 481–484. doi:10.1109/IHMSC.2009.243.

[219] W. Zhao, C. Underwood, Robust transition control of a martian coaxial tiltrotor aerobot, Acta Astronautica 99 (2014) 111–129. doi:https://doi.org/10.1016/j.actaastro.2014.02.020.
URL http://www.sciencedirect.com/science/article/pii/S0094576514000770

[220] Z. Sun, R. Wang, W. Zhou, Finite-time stabilization control for the flight mode transition of tiltrotors based on switching method, in: 2017 29th Chinese Control And Decision Conference (CCDC), 2017, pp. 2049–2053. doi:10.1109/CCDC.2017.7978853.

[221] D. Pucci, Towards a Unified Approach for the Control of Aerial Vehicles, Ph.D. thesis, University of Nice Sophia Antipolis, and of Roma (2013).

[222] Dai Chao, Bai Huihui, Zeng Jianping, Nonlinear stabilization control of tilt rotor UAV during transition flight based on HOSVD, in: 2016 IEEE Chinese Guidance, Navigation and Control Conference (CGNCC), 2016, pp. 154–159. doi:10.1109/CGNCC.2016.7828775.

[223] Youngshin Kang, Bumjin Park, Changsun Yoo, Yushin Kim, Samok Koo, Flight test results of automatic tilt control for small scaled tilt rotor aircraft, in: 2008 International Conference on Control, Automation and Systems, 2008, pp. 47–51. doi:10.1109/ICCAS.2008.4694527.

[224] Etkin, Dynamics of Flight, John Wiley and Sons, 1996.

[225] G. Naus, Gain scheduling robust design and automated tuning of automotive controllers, Tech. rep., University of Technology Eindhoven (2009).
URL http://www.mate.tue.nl/mate/pdfs/11022.pdf

[226] M. Kuang, J. Zhu, W. Wang, Y. Tang, Flight controller design and demonstration of a thrust-vectored tailsitter, in: 2017 IEEE International Conference on Robotics and Automation (ICRA), 2017, pp. 5169–5174. doi:10.1109/ICRA.2017.7989605.

[227] Cakici, Modeling, stability analysis and control system design of a small-sized tiltrotor UAV, Master's thesis, Middle East Technical University (2009).
URL http://citeseerx.ist.psu.edu/viewdoc/download?doi=10.1.1.461.7922&rep=rep1&type=pdf

[228] X. P. Zhu, Y. H. Fan, J. Yang, Design of tiltrotor flight control system using fuzzy sliding mode control, in: 2010 International Conference on Measuring Technology and Mechatronics Automation, Vol. 1, 2010, pp. 1060–1063. doi:10.1109/ICMTMA.2010.211.

[229] Y. Shtessel, C. Edwards, L. Fridman, A. Levant, Sliding Mode Control and Observation, 2014, pp. 291–320. doi:10.1007/978-0-8176-4893-0_8.

[230] P. Ioannou, J. Sun, Robust Adaptive Control, Dover Books on Electrical Engineering, 1995.

[231] N. Hovakimyan, C. Cao, E. Kharisov, E. Xargay, I. M. Gregory, L1 adaptive control for safety-critical systems, IEEE Control Systems Magazine 31 (5) (2011) 54–104. doi:10.1109/MCS.2011.941961.

[232] C. Cao, N. Hovakimyan, Design and analysis of a novel L1 adaptive controller, part i: control signal and asymptotic stability, in: American Control Conference, Minneapolis, MN, 2006, pp. 3397–3402. doi:10.1109/ACC.2006.1657243.

[233] C. Cao, N. Hovakimyan, Design and analysis of a novel L1 adaptive control architecture, part ii: guaranteed transient performance, in: American Control Conference, Minneapolis, MN, 2006, pp. 3403–3408. doi:10.1109/ACC.2006.1657244.

[234] S. Snyder, P. Zhao, N. Hovakimyan, Adaptive control for linear parameter-varying systems with application to a vtol aircraft, Aerospace Science and Technology 112 (2021) 106621. doi:https://doi.org/10.1016/j.ast.2021.106621.
URL https://www.sciencedirect.com/science/article/pii/S1270963821001310

[235] A. Yatsun, B. Lushnikov, O. Emelyanova, Motion control automation in the quadcopter convertiplane in a transient mode, in: 2018 International Russian Automation Conference (RusAutoCon), 2018, pp. 1–6. doi:10.1109/RUSAUTOCON.2018.8501649.

[236] Changjie Yu, Jihong Zhu, Zengqi Sun, Nonlinear adaptive internal model control using neural networks for tilt rotor aircraft platform, in: Proceedings of the 2005 IEEE Midnight-Summer Workshop on Soft Computing in Industrial Applications, 2005. SMCia/05., 2005, pp. 12–16. doi:10.1109/SMCIA.2005.1466940.

[237] M. Zeilinger, Model predictive control, Class Lecture, lecture Notes (2019).

[238] X. Yang, L. Dong, W. Liaoni, S. Yangyang, Design and implementation of twin-rotor tail-sitter UAV, in: 2015 IEEE Advanced Information Technology, Electronic and Automation Control Conference (IAEAC), 2015, pp. 406–410. doi:10.1109/IAEAC.2015.7428584.

[239] R. Naldi, L. Marconi, On robust transition maneuvers for a class of tail-sitter vehicles, in: 49th IEEE Conference on Decision and Control (CDC), 2010, pp. 358–363. doi:10.1109/CDC.2010.5717170.

[240] Y. Nakamura, A. Arakawa, K. Watanabe, I. Nagai, Transitional flight simulations for a tilted quadrotor with a fixed-wing, in: 2018 IEEE International Conference on Mechatronics and Automation (ICMA), 2018, pp. 1829–1836. doi:10.1109/ICMA.2018.8484666.

[241] F. Cakici, K. Leblebicioglu, Modeling and simulation of a small-sized tiltrotor UAV, The Journal of Defense Modeling and Simulation: Applications, Methodology, Technology 9 (2012) 335–345. doi:10.1177/1548512911414951.

[242] J. Apkarian, Pitch-decoupled VTOL/FW aircraft: First flights, in: 2017 Workshop on Research, Education and Development of Unmanned Aerial Systems (RED-UAS), 2017, pp. 258–263. doi:10.1109/RED-UAS.2017.8101676.

[243] R. Chiappinelli, M. Cohen, M. Doff-Sotta, M. Nahon, J. R. Forbes, J. Apkarian, Modeling and control of a passively-coupled tilt-rotor vertical takeoff and landing aircraft, in: 2019 International Conference on Robotics and Automation (ICRA), 2019, pp. 4141–4147. doi:10.1109/ICRA.2019.8793606.

[244] G. Francesco, E. D´Amato, M. Mattei, INDI Control with Direct Lift for a Tilt Rotor UAV, IFAC-PapersOnLine 48 (2015) 156–161. doi:10.1016/j.ifacol.2015.08.076.

[245] T. A. Johansen, T. I. Fossen, Control allocation-a survey, Automatica 49 (5) (2013) 1087–1103. doi:https://doi.org/10.1016/j.automatica.2013.01.035.
URL http://www.sciencedirect.com/science/article/pii/S0005109813000368

[246] R. D'Sa, N. Papanikolopoulos, Design and Experiments for MultI-Section-Transformable (MIST)-UAV, in: 2019 International Conference on Robotics and Automation (ICRA), 2019, pp. 1878–1883. doi:10.1109/ICRA.2019.8793575.

[247] J. Apkarian, Attitude control of pitch-decoupled VTOL fixed wing tiltrotor, in: 2018 International Conference on Unmanned Aircraft Systems (ICUAS), 2018, pp. 195–201. doi:10.1109/ICUAS.2018.8453473.

[248] R. Takeuchi, K. Watanabe, I. Nagai, Development and control of tilt-wings for a tilt-type quadrotor, in: 2017 IEEE International Conference on Mechatronics and Automation (ICMA), 2017, pp. 501–506. doi:10.1109/ICMA.2017.8015868.

[249] L. M. Sánchez-Rivera, R. Lozano, A. Arias-Montano, Pitching moment analysis and adjustment for tilt-wing UAV in VTOL mode, in: 2019 International Conference on Unmanned Aircraft Systems (ICUAS), 2019, pp. 1445–1450. doi:10.1109/ICUAS.2019.8797952.